ARTICLE IN PRESS
CHEMGE-18218; No of Pages 9
Chemical Geology xxx (2017) xxx–xxx
Contents lists available at ScienceDirect
Chemical Geology
journal homepage: www.elsevier.com/locate/chemgeo

Factors constraining the geographic distribution of earthquake geochemical and fluid-related precursors

Giovanni Martinelli [a,*], Andrea Dadomo [b]

[a] ARPAE Environmental Protection Agency of Emilia Romagna Region, Via Amendola 2, 42100 Reggio Emilia, Italy
[b] GEOINVEST Srl, Via della Conciliazione 45/A, 29122 Piacenza, Italy

ARTICLE INFO

Article history:
Received 29 July 2016
Received in revised form 5 January 2017
Accepted 8 January 2017
Available online xxxx

Keywords:
Earthquake precursor
Earthquake prediction
Geochemical anomaly
Tectonic pumping
Natural strainmeter

ABSTRACT

Earthquake precursors are elusive, and this elusiveness has hampered earthquake prediction. In this paper, the available catalogues of historical and contemporary geochemical and fluid-related precursors of earthquakes are considered.
The locations of recording sites are mapped and compared with data concerning volcanic locations, heat flows, crustal velocities and the depth of seismic events. Possible relations among the considered geophysical parameters and the occurrence of fluid-related earthquake precursors are discussed. Only some geological and geophysical conditions may allow for the occurrence of fluid-related earthquake precursory phenomena. As a consequence, the geophysical models utilized to explain the occurrence of earthquake precursors should be updated. Furthermore, only some areas of the world are deemed suitable for earthquake fluid-related precursor monitoring.

1. Introduction

Possible precursory non-seismometric earthquake phenomena have attracted the attention of researchers for many centuries. These phenomena have been registered in historical records and considered in research oriented towards earthquake prediction experiments (Howell, 1986; Martinelli, 2000). During pioneering research carried out in the period of 1800–1950, single parameters or clusters of parameters deemed responsible for observed precursory phenomena were identified. During the 1960s, research projects into earthquake precursors started in Japan, China, the former USSR and the USA. Contrasting results were obtained, and after 1985, new more comprehensive multiparametric experiments were launched in Turkey (Berkhemer et al., 1990; Yuce and Ugurluoglu, 2003), the USA (Bakun and Lindh, 1985), Japan (Uyeda, 2013), the former Soviet Union (Sidorin, 2003), China (Zhang et al., 2013), Iceland (Stefánsson, 2011), Taiwan (Walia et al., 2009; Chen et al., 2015), etc. As a consequence, in the past few decades, many possible earthquake precursors have been utilized in research to describe and understand the physical and chemical processes occurring in the Earth's crust in the phases preceding earthquakes. A portion of the considered parameters are related to underground fluids. Fluid parameters are still widely studied in this kind of research owing to their physical and chemical peculiarities. For instance, groundwater is incompressible; thus, it may act as a natural strainmeter when an aquifer is confined (Bodvarsson, 1970; Roeloffs, 1988; Yaltirak et al., 2005; Yuce et al., 2010). The chemical composition of the groundwaters may provide interesting information about fluid movements in the crust. Gases may provide information about deep fluid migration processes towards the earth's surface (e.g. Thomas, 1988). Such information is not detectable by means of other geophysical parameters. As a consequence, underground fluid monitoring has been carried out jointly with other geophysical parameters. The idea to simultaneously monitor a variety of parameters, including deep originated fluids, was first put forward by Galitzin in 1911 (Zarkov, 1986) following publications by Michele Stefano De Rossi (De Rossi, 1879; De Rossi, 1884), and the complete works of Boris Borisovich Galitzin were published in 1960 (Galitzin, 1960; in pages 426–427 of vol.2 some recommendations about geofluid monitoring are published; an excerpt is shown in Fig. S.3 in the Supplementary material). This idea became predominant in almost all modern research projects on earthquake precursors. In particular, researchers involved in modern research projects consider that dynamic of deep fluids can be influenced by crustal deformative processes. Hence, geochemical and hydrogeologic data are compared with data related to crustal deformation, such as GPS data, seismicity, and satellite data. Fluid-related possible precursory phenomena are not always detectable (Kumpel, 1992). Many earthquakes occur in areas where underground fluids are inaccessible. In other cases, manual or automatic monitoring systems fail because no anomalous signal is recorded prior to the earthquakes. Thus, fluid-related precursors are elusive, as are many other possible earthquake precursors, and currently cannot predict earthquakes (e.g., Jordan et al., 2011). Sometimes possible

* Corresponding author.
E-mail address: giovanni.martinelli15@gmail.com (G. Martinelli).

http://dx.doi.org/10.1016/j.chemgeo.2017.01.006

fluid-related precursory signals are very clear, and researchers have tried to replicate the experience in other places; however, the results are rarely convincing. The purpose of the present work is to identify the possible existence of constraint factors capable of limiting the natural possibilities to generate eventual fluid-related precursory signals. The possibility of generating possible fluid-related precursory signals could depend on the geological context and the local geophysical conditions (e.g., Rigo, 2010). A review of possible favourable and unfavourable geophysical conditions has been carried out.

2. Catalogues of precursory signals

The need to understand when and where possible precursory phenomena have occurred has obliged contemporary researchers to compile catalogues containing metadata of previous publications (e.g., Cicerone et al., 2009). Catalogues of historical precursory phenomena are still very rare because historical seismologists usually pay attention to parameters related to the intensity and to the localization of the studied earthquakes. Historical seismologists usually study or review historical records about earthquakes of the past. In this way, catalogues of historical earthquakes have been compiled for the whole world (e.g., Albini et al., 2014 and references therein). Catalogues of the environmental effects of contemporary earthquakes usually report data about geofluids (e.g., Serva et al., 2011 and references therein), but, in general, information about possible earthquake precursors in historical seismic events are few and far between. Martinelli (1997) published a preliminary catalogue of possible precursory phenomena that occurred in Italy in the period of 1117–1980. This catalogue was recently reviewed and is available in the Supplementary material. Other catalogues considering recent earthquakes and related precursory phenomena have been compiled by different authors. In particular, Hauksson (1981) reviewed all the available radon precursory anomalies throughout the world published in the period of 1971–1981. Friedmann (1985) reviewed all available radon precursory anomalies published in the period of 1969–1982. Toutain and Baubron (1999) reviewed the gaseous anomalies published in the period of 1980–1995. Kissin and Grinevsky (1990) reviewed the available anomalies in water level data in the period of 1948–1980. Hartmann and Levy (2005) reviewed gaseous and water-related anomalies published in the period of 1978–1997. Cicerone et al. (2009) reviewed the geochemical, hydrogeological and geophysical anomalies that occurred in the period of 1948–2001. Ghosh et al. (2009) reviewed radon data recorded in many parts of the world in the period of 1983–2002. Petraki et al. (2015) reviewed radon data recorded all around the world in the period of 1966–2014. Woith (2015) reviewed radon data recorded all round the world in the period of 1967–2014. All the above-mentioned authors directly or indirectly recognized that crustal deformative processes (see also Bernard, 2001; Wang and Manga, 2010) are responsible for observed anomalies in geofluids; thus, further catalogues of geophysical precursors related to crustal deformations could be useful for understanding fluid anomalies recorded before earthquakes. Roeloffs (2006) reviewed precursory deformative anomalies published in the period of 1979–2004, whereas Cicerone et al. (2009) reviewed, among other things, precursory ground deformation anomalies published in the period of 1974–1999.

3. Maps of locations where precursors were detected

3.1. A catalogue and a map of historical earthquake precursors of Italy

The catalogue of non-seismometric precursory phenomena of Italy (Table S.1 in Supplementary material) considers all physico-chemical variations in geofluids that occurred in Italy in concomitance with earthquakes, according to Bonito (1691), De Rossi (1879), Mercalli (1883), Baratta (1901) and Boschi et al. (1995), in the period of 1117–1980. Approximately 400 earthquakes were considered, but only a few were really preceded by significant anomalies in geofluids. In particular, geochemical and geophysical anomalies were detected in the Island of Ischia (southern Italy) before the 1881 and 1883 earthquakes (Mercalli, 1883; De Rossi, 1884; Boschi et al., 1995; Molin et al., 2003). In 1883, the level of the sea water significantly lowered some days before the mainshock; thus, a possible crustal deformation phenomenon (uplift) was observed (De Rossi, 1884; see also Carlino, 2012). Fig. 1 is a map that includes all locations in Italy where geofluids were upset by earthquakes during historical times and locations where precursory anomalies in geofluids were detected jointly with ground deformations. The close relationship among fluid-related phenomena and crustal deformation processes has led to the need to map all the fluid-related precursory phenomena and all precursory deformative processes reviewed by the aforementioned authors in present research.

3.2. A catalogue and a map of contemporary earthquake precursors of the world

All the catalogues of publications considered by Hauksson (1981), Friedmann (1985), Toutain and Baubron (1999), Kissin and Grinevsky (1990), Hartmann and Levy (2005), Roeloffs (2006), Ghosh et al. (2009), Cicerone et al. (2009), Petraki et al. (2015), and Woith (2015) were reviewed and merged. All duplicates were removed and a catalogue. Available references about groundwater level changes, temperature changes, geochemical variations in gas emissions and ground deformations were obtained (Table S.2 in Supplementary material). Data on the locations where precursory phenomena were observed were obtained by reviewing the publications listed in Table S.2 (Supplementary material). A map including all the considered locations is shown in Fig. 2.

4. Geophysical common characteristics of monitoring sites where precursory signals were recorded

A significant number of monitoring sites where precursory phenomena were observed are located in areas where a relatively high heat flow was measured. These areas are characterized by intense deep fluid circulation, which also influences the mechanical characteristics of the lithospere (Ranalli and Rybach, 2005). A map including heat flow values (Goutorbe et al., 2011), Holocenic and Pleistocenic active volcanoes (Siebert et al., 2010 and references therein) and locations where precursors were observed is shown in Fig. 3.

Meanwhile, a significant number of precursory crustal deformation phenomena were detected at the boundaries of tectonic plates; thus, a map is shown in Fig. 4 to better display the strain velocity values of tectonic motion compiled by Kreemer et al. (2003) (see also Kreemer et al., 2014). In particular, the 2nd invariant parameter calculated by Kreemer et al. (2003) appears relatively high in some tectonically active areas simultaneously affected by high heat flow values. Ranalli and Murphy (1987) and Ranalli and Rybach (2005) found that various kinds of crust are possible. The mechanical behaviour of a lithosperic body is controlled by the nature of the stress regime (tensional or compressional), the strain rate, the petrological composition of the lithospheric rocks, the temperature profile and the pore fluid pressure. Crustal mechanical characteristics imply rheological stratifications. In particular, the brittle/ductile transition is shallower in areas characterized by high heat flow values. Chen and Molnar (1983) found that in regions affected by high geothermal anomalies, the maximum focal depths are shallow and most of the seismicity occurs within the first 15 km.

To describe shallower seismicity, the most updated and reviewed worldwide catalogue of instrumental seismicity compiled by the International Seismological Centre (Storchak et al., 2013) was considered. The determination of earthquakes' hypocentral depth can sometimes be a critical parameter (Bondar et al., 2015). Hence, for the sake of simplicity, all earthquakes characterized by $M \geq 4.95$ that occurred within a depth of 20 km are mapped in Fig. 5 and compared to the heat

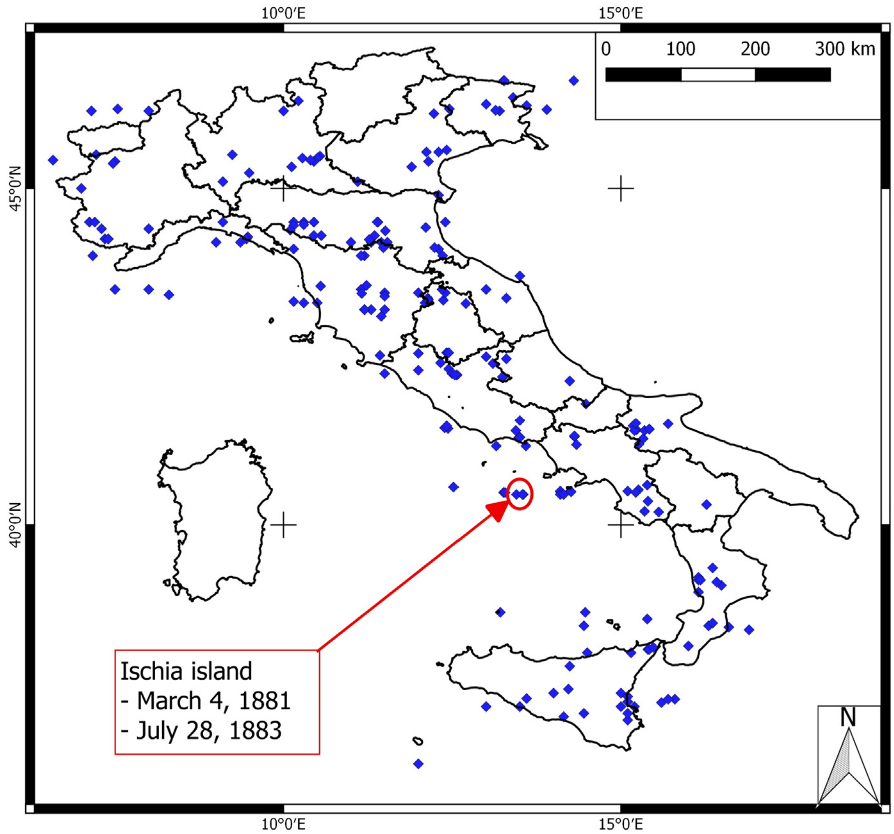

Fig. 1. Map of all sites where phenomena reported in Table S.1 occurred. In the Island of Ischia (southern Italy), fluid-related precursory phenomena were observed in 1881 and in 1883 (De Rossi, 1884; Molin et al., 2003). De Rossi (1884) also reported precursory ground deformations observed before the earthquake of 1883. The seismic event that occurred in 1881 was characterized by Me = 5.4, whereas the event occurred in 1883 was characterized by Me = 5.8 (Rovida et al., 2011).

flow values and to the 2nd invariant values previously considered (Fig. 6).

Approximately all the crustal deformative and fluid-related precursory phenomena occurred in areas characterized by the following parameters:

a) heat flux > 60 mW/m^2
b) 2nd Invariant > 5 yr^{-1}
c) depth of a significant part of local earthquakes < 20 km. These areas are characterized by relatively shallow seismicity.

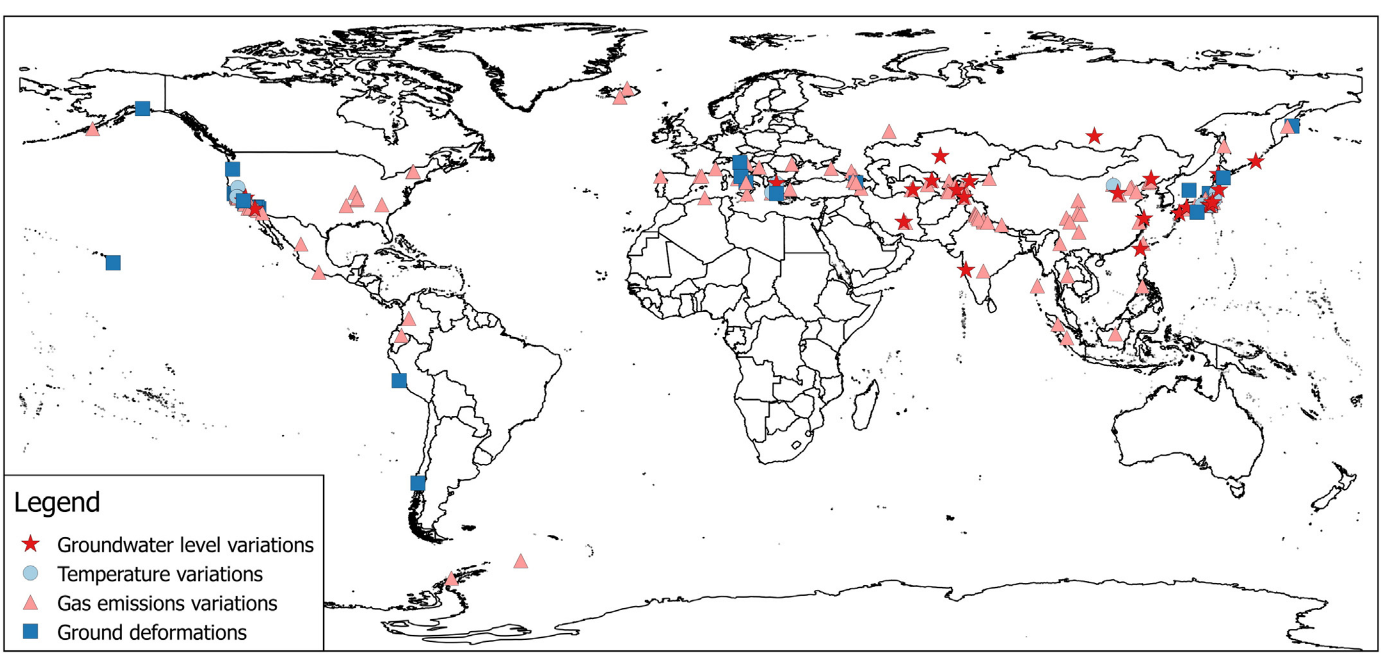

Fig. 2. Map of fluid-related and ground deformation precursory phenomena reported in Table S.2 (Supplementary material). These phenomena were described in a variety of papers reviewed by Hauksson (1981), Friedmann (1985), Toutain and Baubron (1999), Kissin and Grinevsky (1990), Hartmann and Levy (2005), Roeloffs (2006), Ghosh et al. (2009), Cicerone et al. (2009), Petraki et al. (2015), and Woith (2015).

Please cite this article as: Martinelli, G., Dadomo, A., Factors constraining the geographic distribution of earthquake geochemical and fluid-related precursors, Chem. Geol. (2017), http://dx.doi.org/10.1016/j.chemgeo.2017.01.006

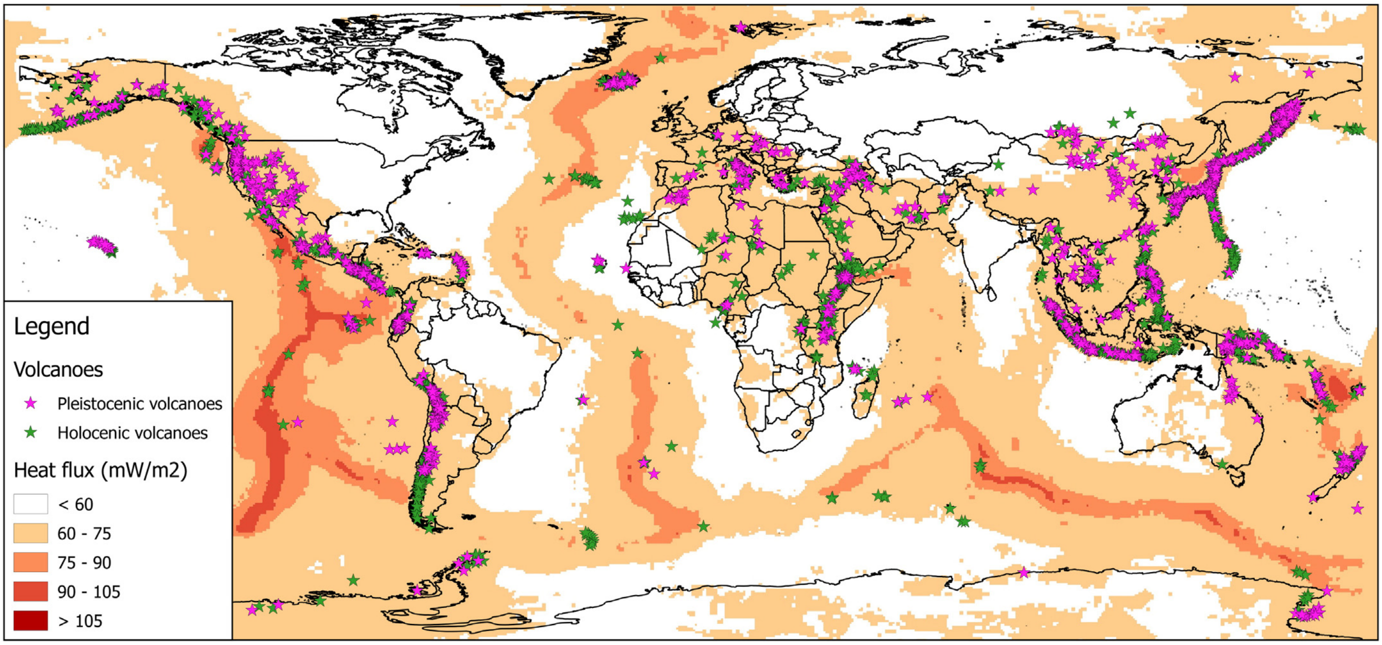

Fig. 3. Map of heat flux values (Goutorbe et al., 2011) and locations of volcanoes active during the Holocenic and Pleistocenic epochs (Siebert et al., 2010). The highest heat flux values are often observed in volcanic or in geothermal areas.

Hence, geophysical constraint factors indicating a soft crust capable of hosting geofluids and shallow depth earthquakes could also be considered key prerequisites for research oriented towards the detection of possible earthquake precursors.

5. Geochemical and geophysical implications for geofluid monitoring

5.1. The monitoring of incompressible fluids

Possible deep fluid pressure variations due to crustal deformations are considered proportional to the stress and volumetric strain. The stress-strain relationship for an isotropic, linearly elastic porous medium was proposed by Rice and Cleary (1976). The stress tensor σ_{kk}, the volumetric strain ε_{kk} and the fluid pressure p under undrained conditions have been described as follows:

$$p = -B\sigma_{kk}/3 \quad (1)$$

$$p = -2GB(1+\nu_u)\varepsilon_{kk}/3(1+\nu_u) \quad (2)$$

where G is the shear modulus, B is the Skempton coefficient, and ν_u is the Poisson's ratio under undrained conditions. Groundwater can be utilized as natural strainmeters, with water being incompressible. Fluid pressure is proportional to the stress and volumetric strain. In particular, the water level can be utilized as the signal of a natural sensitive (10^{-7}–

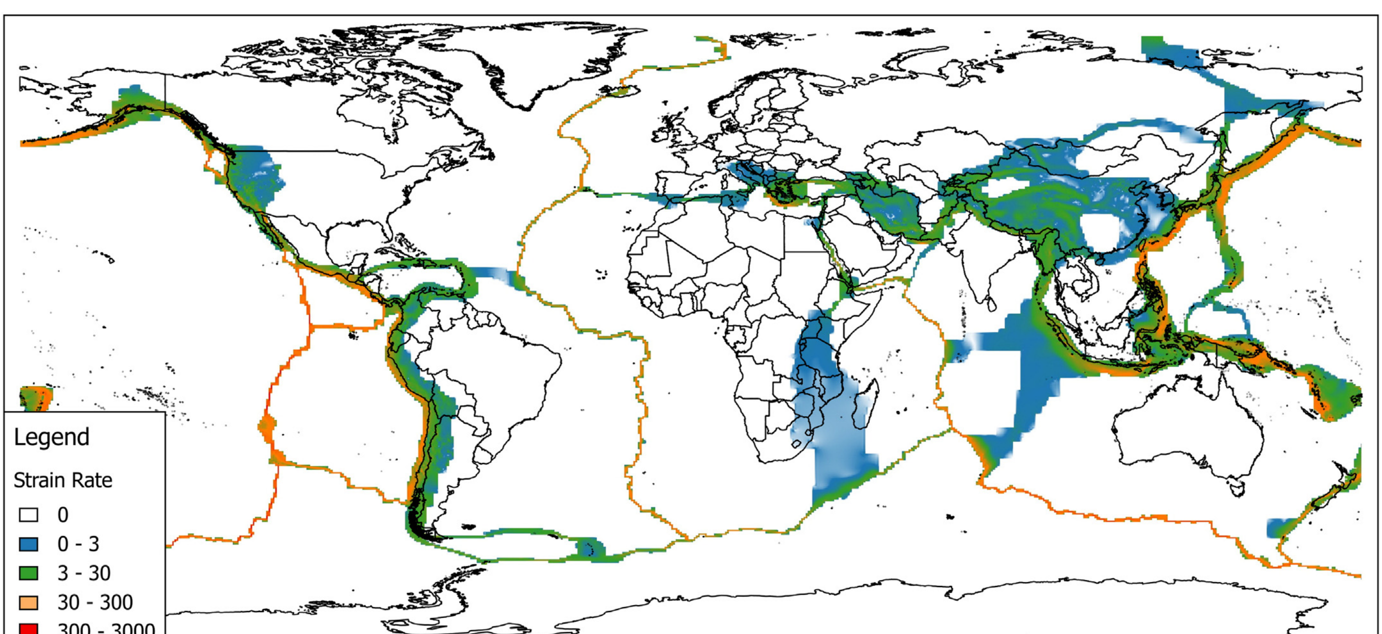

Fig. 4. Strain rate field (2nd invariant 10^{-9} yr^{-1}) according to Kreemer et al. (2003).

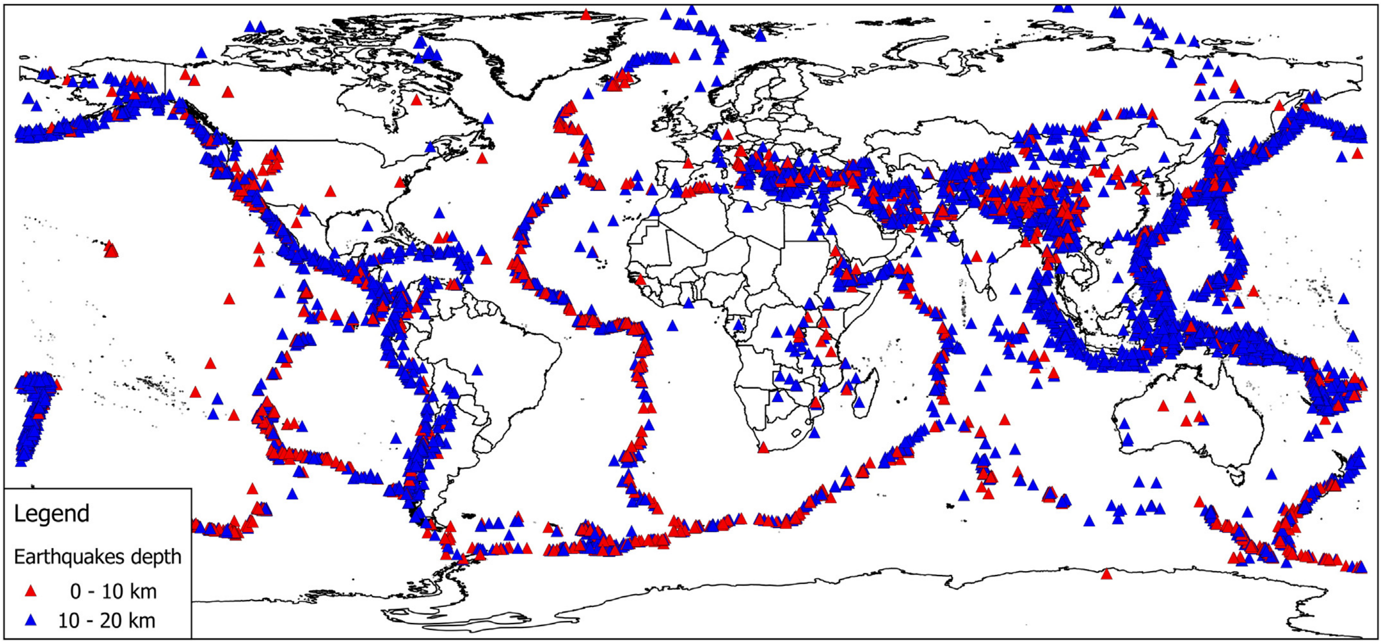

Fig. 5. Map of the epicentral locations of earthquakes characterized by M ≥ 5 that occurred in the depth intervals 0–10 km and 10–20 km according to the ISC Catalogue (Storchak et al., 2013).

Fig. 6. Graphs of earthquakes that occurred throughout the world in the period of 1900–2009 according to the ISC Catalogue (Storchak et al., 2013). Earthquakes are represented by dots in the four graphs. Each graph considers their depth, local heat flux (Goutorbe et al., 2011) and strain rate (Kreemer et al., 2003). Shallower seismic events occur in areas characterized by a relatively high heat flux. Shallower seismic events in the upper right hand corner are localized in mid-oceanic ridges.

Please cite this article as: Martinelli, G., Dadomo, A., Factors constraining the geographic distribution of earthquake geochemical and fluid-related precursors, Chem. Geol. (2017), http://dx.doi.org/10.1016/j.chemgeo.2017.01.006

10^{-8}) strainmeter when deformative processes are ongoing in an earthquake candidate area (e.g., Matsumoto et al., 2007 and references therein).

5.2. The monitoring of compressible fluids

The most relevant gases involved in the Earth's degassing are CH_4 and CO_2. These gases are also responsible for water-gas-rock interaction processes, which may change the cation and anion concentration in the composition of groundwaters. Aquifer mixing processes (e.g., Thomas, 1988) may also induce temperature variations of geofluids as well as chemical variations in dissolved ions utilized as possible earthquake precursors (e.g., Skelton et al., 2014). Possible precursory variations observed in radon and helium can be considered to be determined by changes in the carrier gas composition due to possible mixing phenomena and to gas-water-rock interactions. Radon variations in geothermal systems have also been attributed to flow rate variations (e.g., D'Amore and Sabroux, 1976), which could be induced by strain in geological formations. Gases are compressible; thus, radon or helium data are not easily comparable with strainmeter data and the calculation of a stress tensor from radon data remains an unsolved problem (e.g., Roeloffs, 1999). Nevertheless, tectonic reactivation may be revealed by pressure variations of deep gases possibly tracked by radon and by other jointly monitored geochemical and environmental parameters. Helium isotopes may give first-hand information about very deep tectonic processes (Mamyrin et al., 1980). Barry et al. (2009) experimented with high-rate $^3He/^4He$ sampling equipment capable of acquiring detailed knowledge of fluid evolution in deep geological environments. Compressible fluids may reveal eventual stress variation processes at depth.

5.3. Fluid-related precursors models in earthquake prediction studies

Fluid-related precursors have been widely utilized in earthquake prediction research. In such research, the determination of the time and location of an eventual forthcoming earthquake is crucial (e.g., Dobrovolsky et al., 1979). These equations consider the distance between the epicenter and the geochemical monitoring site. In some cases, the amplitude, frequency and duration of recorded signals are also considered. Etiope et al. (1997) reviewed available equations in the scientific literature capable of linking, in principle, geochemical data with the time of the occurrence, size and location of forthcoming earthquakes. All considered equations were related to the so-called Dilatancy Models (e.g., Scholz, 2002 and references therein). These models imply that pore fluid possible variations are generated in rock volumes close to the hypocenter of a forthcoming seismic event. Nucleation processes of earthquakes last only a few seconds (Ellsworth and Beroza, 1995); thus, eventual fluid-related precursory signals observed weeks or days before mainshock could not be originated by fast nucleation phases. Furthermore, the rock thickness between a nucleating seismic event and the Earth's surface could be a strong obstacle. In this sense, eventual fluid-related precursory phenomena are not satisfactorily explained by equations reviewed by Etiope et al. (1997). Roeloffs (2006) found that eventual precursory crustal deformation processes correspond to only a small fraction of the total crustal strain due to the occurrence of a seismic event. In the meantime, all the crustal layers of a deforming crustal volume are involved in intense geothermal fluid circulations, as described in point 4. As a consequence, significant hydrogeological and geochemical pore pressure variations could be generated independently from the forthcoming hypocentral rock volume. Deep pore pressure variations may contribute to the total crustal strain processes and may trigger one or more contemporary earthquakes observed at the Earth's surface by suitable geofluid sensors. In this sense, the preparatory stages of a seismic event are as follows:

1) a crustal deformation process starts
2) a significant crustal volume is affected by pore pressure variations capable of being detected at the surface by eventual suitable equipment
3) one or more seismic events are nucleated by the crustal deformation process and by pore fluid variations at depth
4) one or more significant earthquakes may occur
5) or many small seismic events may occur as a consequence of points a) and b).

This interpretation of possible geochemical or hydrogeological precursors does not require Dilatancy Models, which can be utilized to better explain any other variation in different geophysical parameters, such as Vp/Vs and foreshock frequency variations. Furthermore, the possible lack of anomalies could be easily explained as due to anisotropies in the fluid distribution and in rock permeability affecting the geological environment (see also Gleeson and Ingebritsen, 2017).

5.4. Further data elaborations

The available data listed in Table S.2 (Supplementary data) were considered. Crustal deformations may induce water level variations, water temperature variations and geochemical variations in gases. Part of the considered data on gases could be slightly less reliable in comparison to the other considered precursors because they are possibly more affected by meteorological noise, particularly when the measurements are carried out in soils. Thus, only ground deformations, water level variations and water temperature variations were considered. Fig. 7 shows the frequency distribution of considered precursors compared to the strain rate and heat flux. There is not a clear distribution trend of precursory data with the strain rate, whereas 80% of the considered phenomena were observed in places of the world characterized by heat flux values ≥ 60 mW/m^2. All considered phenomena utilized in Fig. 7 occurred in areas characterized by shallow seismicity (Fig. 8). Shallow earthquakes are more effective than deeper ones in inducing ground deformations, particularly in high heat flux areas (Toda, 2011; Tang et al., 2015). The highest frequency of precursors due to ground deformation (ground deformation, water level, water temperature in Fig. 7) was limited to the heat flux interval 60–75 mW/m^2. A significant part of gas-related precursors, as shown in Fig. 2, was recorded in the same high heat flux areas evidenced by Fig. 7; thus, the most significant constraint factors for identifying areas suitable for research oriented towards fluid-related earthquake precursors are as follows:

a) heat flux ≥ 60 mW/m^2
b) seismicity characterized by <20 km depth (Fig. 8)

This implies that shallow crustal deformative processes could be effective in inducing possible fluid-related precursory phenomena; thus, only in some areas of the world can earthquake precursor research be carried out. In some of the areas characterized by a relatively high frequency of M > 5 earthquakes (Japan, California, etc.), research oriented towards the study of possible fluid-related earthquake precursors has been carried out. In other areas, although equally characterized by a relatively high frequency of M > 5 earthquakes such as Chile and Indonesia, fluid-related earthquake precursors have been scarcely studied. They could be considered promising potential test site areas. The present study utilized data bases characterized by world coverage and relatively low resolution, so further constraint factors could be revealed by studies at the local geographic scale.

6. Conclusions

The analysis of catalogues of historical and contemporary fluid-related earthquake precursors revealed that they may occur in particular areas of the world. These areas are affected by strong crustal deformative processes, high heat flow values and shallow seismicity. Fluid-

Please cite this article as: Martinelli, G., Dadomo, A., Factors constraining the geographic distribution of earthquake geochemical and fluid-related precursors, Chem. Geol. (2017), http://dx.doi.org/10.1016/j.chemgeo.2017.01.006

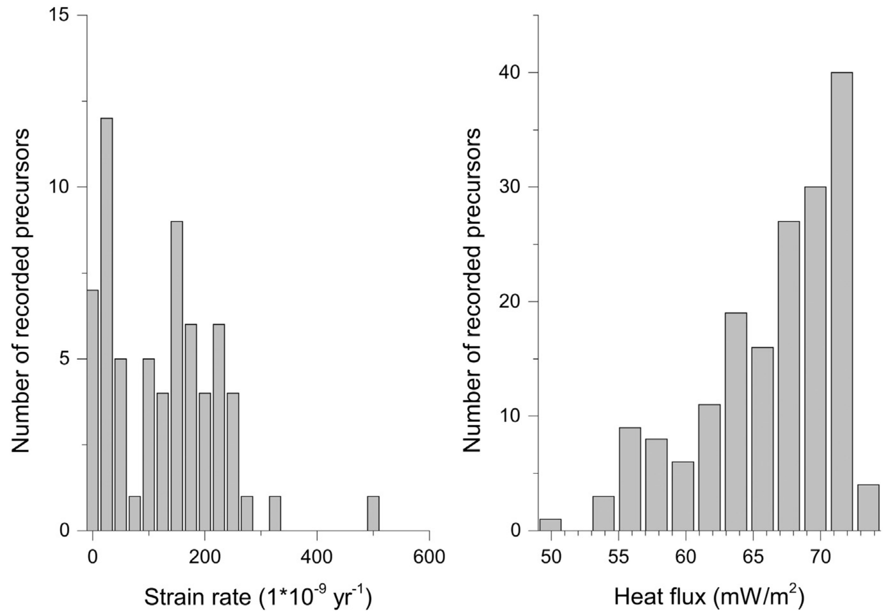

Fig. 7. Graphs of the frequency distributions of precursory phenomena compared to the strain rate (left) and to heat flux (right) occurring in the same places where precursory variations were observed.

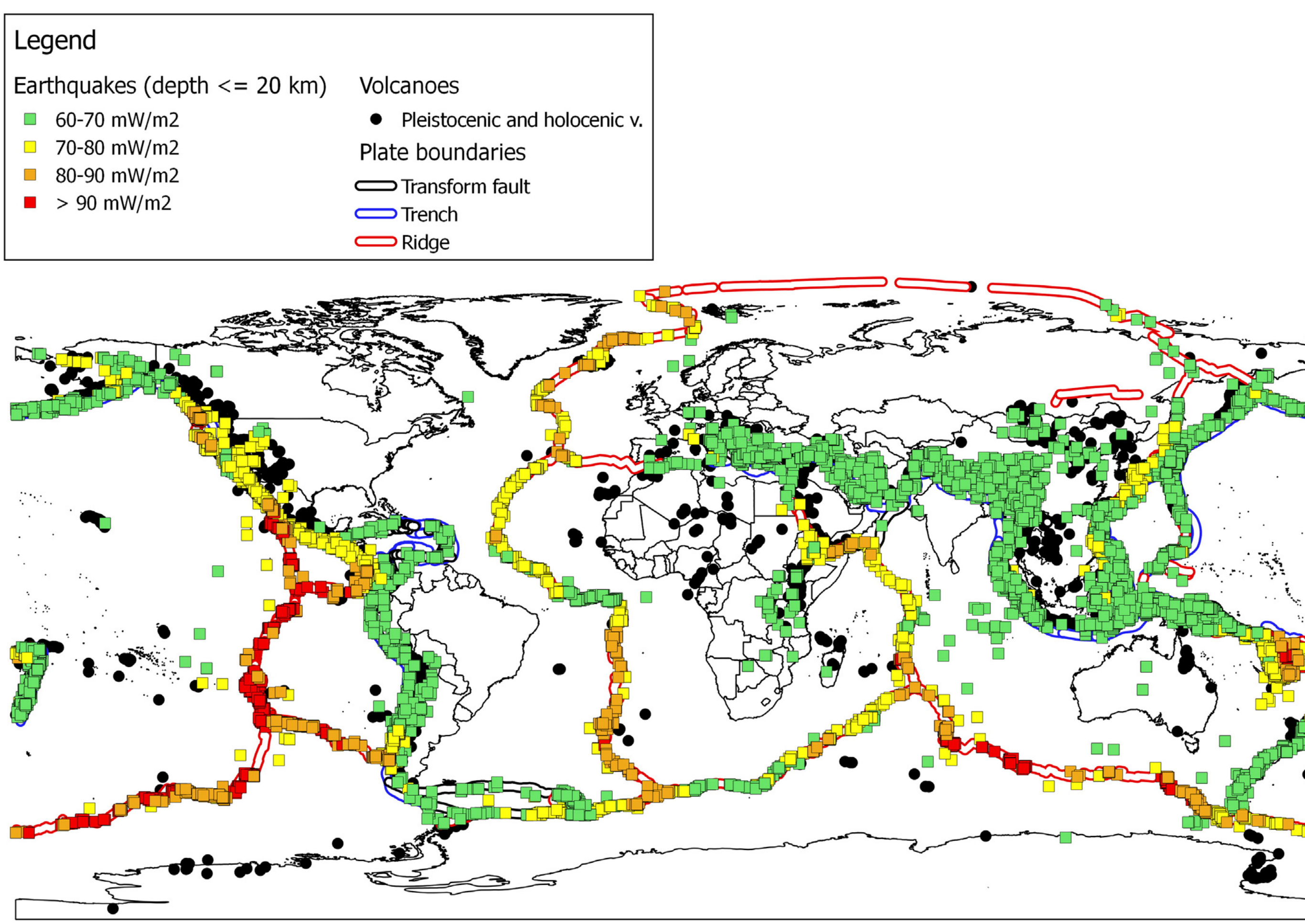

Fig. 8. Image of earthquakes characterized by M ≥ 5 (Bondar et al., 2015) that occurred in areas affected by a relatively high heat flux (≥ 60 mW/m^2) in the depth interval of 0–20 km. Each seismic event is inserted in a pixel (100 ∗ 100 km) indicating the local heat flux (Goutorbe et al., 2011). Pleistocenic and Holocenic volcanic areas (Siebert et al., 2010) are also indicated. Plate boundaries were kept by Coffin et al. (1998). Earthquake precursors that occurred in the considered areas are shown in Fig. 2. Details about depth intervals of 0–10 km and 10–20 km are shown in the Supplementary material (Fig._S_1). Geographic details about the most relevant areas are also available in the Supplementary Material (Fig._S_2).

related earthquake precursors are linked to intense fluid circulation in the deformation of huge rock volumes rather than small hypocentral rock volumes. The lack of one or more of the identified constraint parameters probably limited the possibility of observing eventual earthquake fluid-related precursors in the past. This implies that future research projects on earthquake precursors will be mostly carried out in areas where the detectability of possible precursors is higher. These areas include countries where the research started some decades ago as well as countries where little attention has been paid to possible fluid-related earthquake precursors. Eventual research on earthquake prediction will be affected by the identified constraint factors regarding the detectability of possible geochemical and hydrogeological earthquake precursors. The role of potential natural strainmeters of geofluids has been confirmed.

Supplementary data to this article can be found online at http://dx.doi.org/10.1016/j.chemgeo.2017.01.006.

Acknowledgements

Thanks are due to Anna Skorkina (RAS, Geophysical Survey – Petropavlosk) and to Graziano Ferrari (INGV-Bologna) for suggestions on the archive research and for translations from Russian of excerpts written by Boris Borisovich Galitzin. Thanks are also due to Alberto Comastri (INGV-Bologna) for suggestions on the interpretation of excerpts written by Michele Stefano De Rossi. Thanks are also due to two unknown reviewers who contributed to improving the quality of text. This study has benefited from funding provided by the Italian Presidenza del Consiglio dei Ministri-Dipartimento della Protezione Civile (DPC), Projects S3-2012 and S3-2014-2015. This paper does not necessarily represent the DPC's official opinion and policies. This paper was presented at the 13th International Conference on Gas Geochemistry, Chengdu (China), 2015.

References

Albini, P., Musson, R.M.W., Rovida, A., Locati, M., Gomez Capera, A.A., Viganò, D., 2014. The global earthquake history. Earthquake Spectra 30:607–624. http://dx.doi.org/10.1193/122013EQS297.

Bakun, W.H., Lindh, A.G., 1985. The Parkfield, California, Earthquake Prediction Experiment. Science 229:619–624. http://dx.doi.org/10.1126/science.229.4714.619.

Balderer W., Martinelli G., 1995. Geochemistry of groundwaters and gases occurring in the November 23, 1980 earthquake area (South Italy), Environ. Geochem. Health, Supplement to vol. 16, 147–163.

Baratta, M., 1901. I terremoti d'Italia. Arnaldo Forni Editore (1979, anastatic reprint), Sala Bolognese (951 pp.).

Barry, P.H., Hilton, D.R., Tryon, M.D., Brown, K.M., Kulogonski, J.T., 2009. A new syringe pump apparatus for the retrieval and temporal analysis of helium (SPARTAH) in groundwaters and geothermal fluids. Geol. Geophys. Geosyst. (G-Cubed) 10 (5). http://dx.doi.org/10.1029/2009GC002422,2009.

Berkhemer, H., Zschau, J., Ergunay, O., 1990. The German-Turkish Project on earthquake prediction research, concept and first results. In: Olivera, C.S. (Ed.), Prediction of Earthquakes - Occurrence and Ground Motion. LNEC, Lisbon, pp. 579–601.

Bernard, P., 2001. From the search of "precursors" to the search on "crustal transients". Tectonophysics 338:225–232. http://dx.doi.org/10.1016/S0040-1951(01)00078-6.

Bodvarsson, G., 1970. Confined fluids as strain meters. J. Geophys. Res. 75, 2711–2718.

Bondar, I., Engdahl, E.R., Villasenor, A., Harris, J., Storchak, D., 2015. ISC-GEM: global instrumental earthquake catalogue (1900–2009), II. Location and seismicity patterns. Phys. Earth Planet. Inter. 239:2–13. http://dx.doi.org/10.1016/j.pepi.2014.06.002.

Bonito, M., 1691. Terra tremante. Arnaldo Forni Editore (1980, anastatic reprint), Sala Bolognese (822 pp.).

Boschi, E., Ferrari, G., Gasperini, P., Guidoboni, E., Smriglio, G., Valensise, G. (Eds.), 1995. Catalogo dei forti terremoti in Italia dal 461 a.C. al 1980. ING-SGA, Bologna (973 pp.).

Carlino, S., 2012. The process of resurgence for Ischia Island (southern Italy) since 55 ka: the laccolith model and implications for eruption forecasting. Bull. Volcanol. http://dx.doi.org/10.1007/s00445-012-0578-0.

Chen, W.-P., Molnar, P., 1983. Focal depths of intracontinental and intraplate earthquakes and their implications for the thermal and mechanical properties of the lithosphere. J. Geophys. Res. 88, 4183–4214.

Chen, C.-H., Tang, C.-C., Cheng, K.C., Wang, C.-H., Wen, S., Lin, C.-H., Wen, Y.-Y., Meng, G., Yeh, T.-K., Jan, J.C., Yen, H.Y., 2015. Groundwater-strain coupling before the 1999 Mw 7.6 Taiwan Chi-Chi earthquake. J. Hydrol. 524:378–384. http://dx.doi.org/10.1016/j.jhydrol.2015.03.006.

Cicerone, R.D., Ebel, J.E., Britton, J., 2009. A systematic compilation of earthquake precursors. Tectonophysics 476:371–396. http://dx.doi.org/10.1016/j.tecto.2009.06.008.

Coffin, M.F., Gahagan, L.M., Lawver, L.A., 1998. Present-day plate boundary digital data compilation. University of Texas Institute for Geophysics Technical Report No. 174, p. 5.

Dall'Aglio, M., 1976. Earthquake prediction by hydrogeochemical methods. Rend. Soc. Ital. Mineral. Petrol. 32, 421–436.

D'Amore, F., Sabroux, J.C., 1976. Signification de la présence de radon 222 dans les fluides géothermiques. Bull. Volcanol. 40, 106–115.

De Rossi, M.S., 1879. La Meteorologia Endogena vol. 1. Arnaldo Forni Editore, Sala Bolognese ((2008, anastatic reprint), 359 pp.).

De Rossi, M.S., 1884. Catalogo ragionato e topografico delle notizie di fatto sui terremoti del 28 luglio 1883 ed illustrazione della annessa carta geognostica dell'Isola d'Ischia. Bull. Vulcan. Ital. 11, 131–175.

Dobrovolsky, I.P., Zubkov, S.I., Myachin, V.I., 1979. Estimation of the size of earthquake preparation zones. Pure Appl. Geophys. 117, 1025–1044.

Ellsworth, W.L., Beroza, G.C., 1995. Seismic Evidence for an Earthquake Nucleation Phase.

Etiope, G., Calcara, M., Quattrocchi, F., 1997. Seismogeochemical algorithms for earthquake prediction: an overview. Ann. Geofis. 40:1483–1492. http://dx.doi.org/10.4401/ag-3825.

Friedmann, H., 1985. Anomalies in the radon content of spring water as earthquake precursor phenomena. Earthquake Predict. Res. 1, 179–189.

Galitzin, B.B., 1960. Izbrannie Trudiy (Selected Works, in Russian) vol. 2. Izd-vo, AN SSSR, Moscow.

Ghosh, D., Deb, A., Sengupta, R., 2009. Anomalous radon emission as precursor of earthquake. J. Appl. Geophys. 69:67–81. http://dx.doi.org/10.1016/j.jappgeo.2009.06.001.

Gleeson, T., Ingebritsen, S.E. (Eds.), 2017. Crustal Permeability. John Wiley & Sons, Chichester (451 pp.).

Goutorbe, B., Poort, J., Lucazeau, F., Raillard, S., 2011. Global heat flow trends resolved from multiple geological and geophysical proxies. Geophys. J. Int. 187, 1405–1419.

Hartmann, J., Levy, J.K., 2005. Hydrogeological and gasgeochemical earthquake precursors - a review for applications. Nat. Hazards 34 (3):279–303. http://dx.doi.org/10.1007/s11069-004-2072-2.

Hauksson, E., 1981. Radon content of groundwater as an earthquake precursor: evaluation of worldwide data and physical basis. J. Geophys. Res. 86 (B10), 9397–9410.

Howell, B.F., 1986. History of ideas on the cause of earthquakes. Eos 67, 1323–1326.

Jordan, T.H., Chen, Y.-T., Gasparini, P., Madariaga, R., Main, I., Marzocchi, W., Papadopoulos, G., Sobolev, G., Yamaoka, K., Zschau, J., 2011. Operational earthquake forecasting. Ann. Geophys. 54 (4):315–391. http://dx.doi.org/10.4401/ag-5350.

Kissin, I.G., Grinevsky, A.O., 1990. Main features of hydrogeodynamic earthquake precursors. Tectonophysics 178:277–286. http://dx.doi.org/10.1016/0040-1951(90)90154-Z.

Kreemer, C., Holt, W.E., Haines, A.J., 2003. An integrated global model of present-day plate motions and plate boundary deformation. Geophys. J. Int. 154:8–34. http://dx.doi.org/10.1046/j.1365-246X.2003.01917.x.

Kreemer, C., Blewitt, G., Klein, E.C., 2014. A geodetic plate motion and Global Strain Rate Model. Geochem. Geophys. Geosyst. 15:3849–3889. http://dx.doi.org/10.1002/2014GC005407.

Kumpel, H.-J., 1992. About the potential of wells to reflect stress variations within inhomogeneous crust. Tectonophysics 211 (1):317–336. http://dx.doi.org/10.1016/0040-1951(92)90068-H.

Mamyrin, B.A., Tolstikhin, I.N., Khabarinj, L.V., 1980. $^{3}He/^{4}He$ ratios in earthquake forecasting. Geochem. Int. 16, 42–44.

Martinelli, G., 1997. Non seismometrical precursors observations in Europe: steps of earthquake prediction research. In: Ferrari, G. (Ed.), Proceedings of the Workshop: "Historical Seismic Instruments and Documents: A Heritage of Great Scientific and Cultural Value.". Conseil de l'Europe, Cahiers du Centre Européen de Géodynamique et de Séismologie vol. 13, pp. 195–216.

Martinelli, G., 2000. Contributions to a history of earthquake prediction research. Seismol. Res. Lett. 71:583–588. http://dx.doi.org/10.1785/gssrl.71.5.583.

Matsumoto, N., Kitagawa, Y., Koizumi, N., 2007. Groundwater-level anomalies associated with a hypothetical preslip prior to the anticipated Tokai earthquake: detectability using the groundwater observation network of the Geological Survey of Japan, AIST. Pure Appl. Geophys. 164:2377–2396. http://dx.doi.org/10.1007/978-3-7643-8720-4_2.

Mercalli, G., 1883. Vulcani e fenomeni vulcanici in Italia. Arnaldo Forni Editore, Sala Bolognese ((1981, anastatic reprint), 374 pp.).

Molin, P., Acocella, V., Funiciello, R., 2003. Structural, seismic and hydrotermal features at the border of an active intermittent resurgent block: Ischia Island (Italy). J. Volcanol. Geotherm. Res. 121 (1–2):65–81. http://dx.doi.org/10.1016/S0377-0273(02)00412-2.

Petraki, E., Nikolopoulos, D., Panagiotaras, D., Cantzos, D., Yannakopoulos, P., Nomicos, C., Stonham, J., 2015. Radon-222: a potential short-term earthquake precursor. J. Earth Sci. Clim. Change 6:282. http://dx.doi.org/10.4172/2157-7617.1000282.

Ranalli, G., Murphy, D.C., 1987. Rheological stratification of the lithosphere. Tectonophysics 132, 281–295.

Ranalli, G., Rybach, L., 2005. Heat flow, heat transfer and lithosphere rheology in geothermal areas: features and examples. J. Volcanol. Geotherm. Res. 148 (1–2):3–19. http://dx.doi.org/10.1016/j.jvolgeores.2005.04.010.

Rice, J.R., Cleary, M.P., 1976. Some basic stress diffusion solutions for fluid-saturated elastic porous media with compressible constituents. Rev. Geophys. Space Phys. 14, 227–241.

Rigo, A., 2010. Precursors and fluid flows in the case of the 1996, Ml = 5.2 Saint-Paul-de-Fenouillet earthquake (Pyrenees, France): A complete pre-, co- and post-seismic scenario. Tectonophysics 480 (1–4):109–118. http://dx.doi.org/10.1016/j.tecto.2009.09.027.

Roeloffs, E., 1988. Hydrologic precursors to earthquakes: a review. Pure Appl. Geophys. 126 (2):177–209. http://dx.doi.org/10.1007/BF00878996.

Roeloffs, E., 1999. Radon and rock deformation. Nature 399:104–105. http://dx.doi.org/10.1038/20072.

Roeloffs, E., 2006. Evidence for aseismic deformation rate changes prior to earthquakes. Annu. Rev. Earth Planet. Sci. 34:591–627. http://dx.doi.org/10.1146/annurev.earth.34.031405.124947.

Rovida, A., Camassi, R., Gasperini, P., Stucchi, M., 2011. CPTI11, la versione 2011 del Catalogo Parametrico dei Terremoti Italiani. Milano, Bologna. http://dx.doi.org/10.6092/INGV.IT-CPTI11 (http://emidius.mi.ingv.it/CPTI).

Scholz, C.H., 2002. The Mechanics of Earthquakes and Faulting. Cambridge University Press, Cambridge (471 pp.).

Serva, L., Blumetti, A.M., Esposito, E., Guerrieri, L., Michetti, A.M., Okumura, K., Porfido, S., Reicherter, K., Silva, P.G., Vittori, E., 2011. Earthquake environmental effects, intensity and seismic hazard assessment: the ESI intensity scale and the EEE catalogue. Memorie Descrittive Carta Geologica d'Italia Vol. 97 (112 pp., Rome).

Sidorin, A.Y., 2003. Search for earthquake precursors in multidisciplinary data monitoring of geophysical and biological parameters. Nat. Hazards Earth Syst. Sci. 3:153–158. http://dx.doi.org/10.5194/nhess-3-153-2003.

Siebert, L., Simkin, T., Kimberly, P., 2010. Volcanoes of the World. University of California Press, Berkeley (568 pp.).

Skelton, A., Andrén, M., Kristmannsdòttir, H., Stockmann, G., Morth, C.-M., Sveinbjornsdottir, A., Jonsson, S., Sturkell, E., Gudrunardottir, H.R., Hjartarson, H., Siegmund, H., Kockum, I., 2014. Changes in groundwater chemistry before two consecutive earthquakes in Iceland. Nat. Geosci. 7:752–756. http://dx.doi.org/10.1038/ngeo2250.

Advances in earthquake prediction. In: Stefánsson, R. (Ed.), Research and Risk Mitigation. Springer-Verlag, Berlin Heidelberg (245 pp.).

Storchak, D.A., Di Giacomo, D., Bonder, I., Engdahl, E.R., Harris, J., Lee, W.H.K., Villasenor, A., Bormann, P., 2013. Public release of the ISC-GEM Global Instrumental earthquake catalogue (1900–2009). Seismol. Res. Lett. 84 (5):810–815. http://dx.doi.org/10.1785/0220130034.

Tang, M.-Y., Liu, J., Shao, Y.-X., Wang, P., Yuan, Z.-D., 2015. Analysis about the minimum magnitude earthquake associate with surface ruptures. Dizhen Dizhi 37: 1193–1214. http://dx.doi.org/10.3969/j.issn.0253-4967.2015.04.020.

Thomas, D., 1988. Geochemical precursors to seismic activity. Pure Appl. Geophys. 126: 241–266. http://dx.doi.org/10.1007/BF00878998.

Toda, S., 2011. Paleoseismology. In: Gupta, H. (Ed.), Encyclopedia of Solid Earth Geophysics. Springer, Dordrecht.

Toutain, J.-P., Baubron, J.-C., 1999. Gas geochemistry and seismotectonics: a review. Tectonophysics 304 (1–2):1–27. http://dx.doi.org/10.1016/S0040-1951(98)00295-9.

Uyeda, S., 2013. On earthquake prediction in Japan. Proc. Jpn. Acad. B 89 (9):391–400. http://dx.doi.org/10.2183/pjab.89.391.

Walia, V., Yang, T.F., Hong, W.-L., Lin, S.-J., Fu, C.-C., Wen, K.-L., Chen, C.-H., 2009. Geochemical variation of soil-gas composition for fault trace and earthquake precursory studies along the Hsincheng fault in NW Taiwan. Appl. Radiat. Isot. 67 (10): 1855–1863. http://dx.doi.org/10.1016/j.apradiso.2009.07.004.

Wang, C.-Y., Manga, M., 2010. Earthquakes and Water. Springer-Verlag, Berlin and Heidelberg (225 pp.).

Woith, H., 2015. Radon earthquake precursor: a short review. Eur. Phys. J. Spec. Top. 224 (4):611–627. http://dx.doi.org/10.1140/epjst/e2015-02395-9.

Yaltirak, C., Yalcin, T., Yuce, G., Bozkurtoglu, E., 2005. Water level changes in shallow wells before and after the 1999 Izmit and Düzce earthquakes and comparison with long term water level observations (1999–2004), NW Turkey. Turk. J. Earth Sci. 14 (3), 281–309.

Yuce, G., Ugurluoglu, D., 2003. Earthquake dates and water level changes in wells in the Eskisehir region, Turkey (technical note). Hydrol. Earth Syst. Sci. 7 (5):777–781. http://dx.doi.org/10.5194/hess-7-777-2003.

Yuce, G., Ugurluoglu, Y.D., Nadar, N., Yalcin, H.T., Yaltirak, C., Streil, T., Oeser, V., 2010. Monitoring of earthquake precursors by multi-parameter stations in Eskisehir region (Turkey). Appl. Geochem. 25 (4):572–579. http://dx.doi.org/10.1016/j.apgeochem.2010.01.013.

Zarkov, V.N., 1986. Interior Structure of the Earth and Planets. Harwood Academic Publishers, Chur, Switzerland ((translated from the Russian), 436 pp.).

Zhang, Y., Gao, F., Ping, J., Zhang, X., 2013. A synthetic method for earthquake prediction by multidisciplinary data. Nat. Hazards 69 (2):1199–1209. http://dx.doi.org/10.1007/s11069-011-9961-y.

Please cite this article as: Martinelli, G., Dadomo, A., Factors constraining the geographic distribution of earthquake geochemical and fluid-related precursors, Chem. Geol. (2017), http://dx.doi.org/10.1016/j.chemgeo.2017.01.006

S1.a

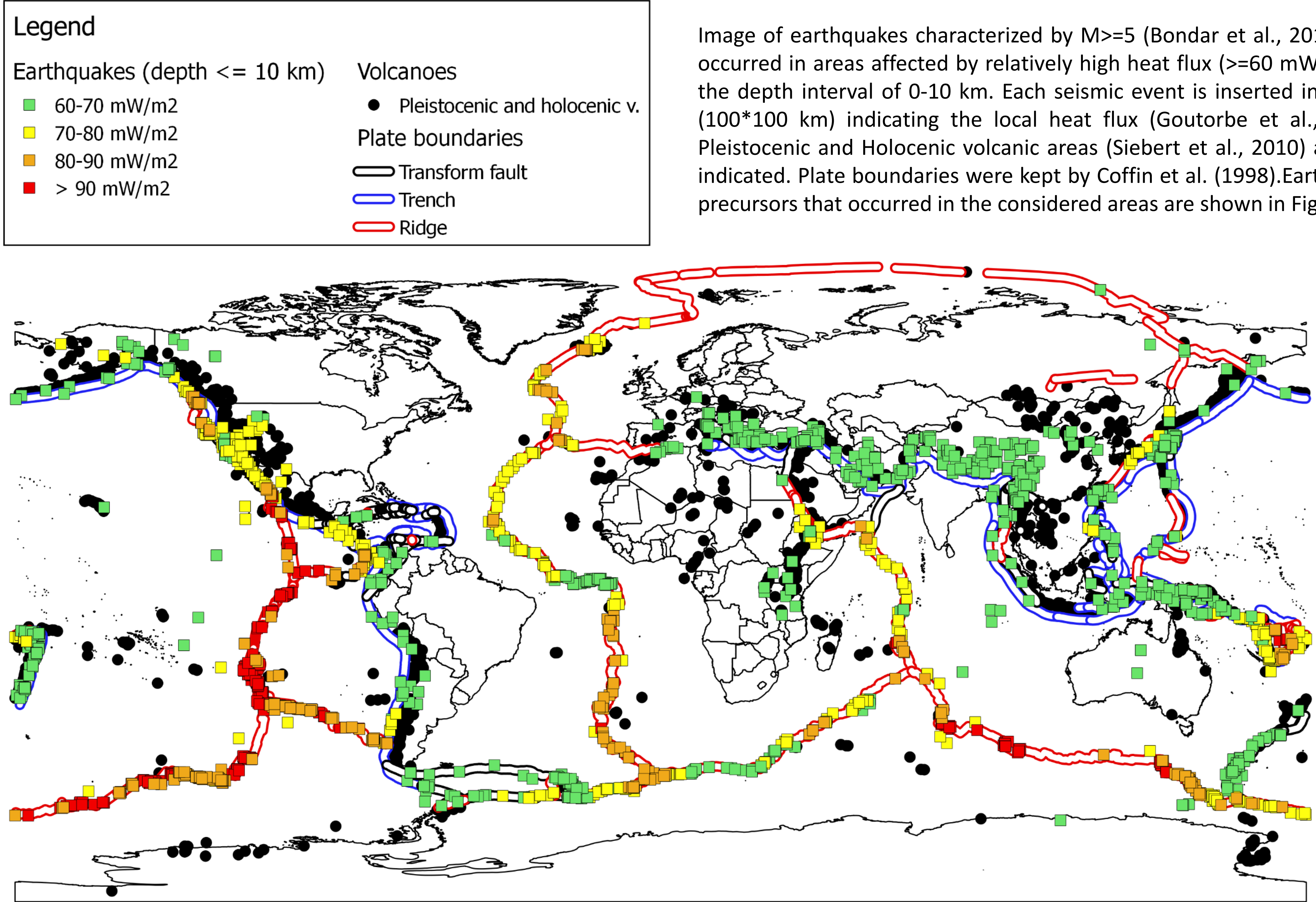

Image of earthquakes characterized by M>=5 (Bondar et al., 2015) that occurred in areas affected by relatively high heat flux (>=60 mW/m2) in the depth interval of 0-10 km. Each seismic event is inserted in a pixel (100*100 km) indicating the local heat flux (Goutorbe et al., 2011). Pleistocenic and Holocenic volcanic areas (Siebert et al., 2010) are also indicated. Plate boundaries were kept by Coffin et al. (1998).Earthquake precursors that occurred in the considered areas are shown in Fig. 2.

S1.b

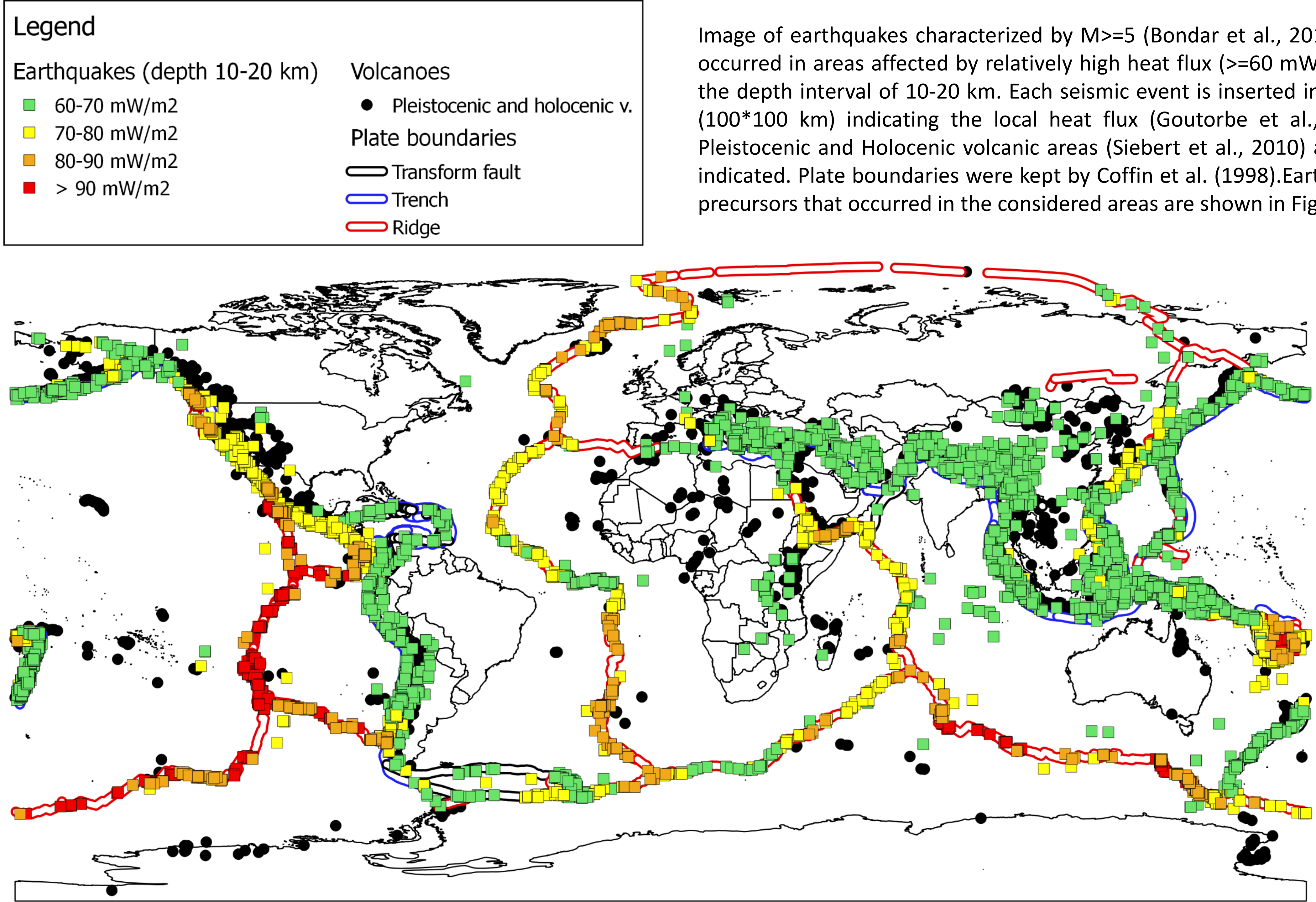

Image of earthquakes characterized by M>=5 (Bondar et al., 2015) that occurred in areas affected by relatively high heat flux (>=60 mW/m2) in the depth interval of 10-20 km. Each seismic event is inserted in a pixel (100*100 km) indicating the local heat flux (Goutorbe et al., 2011). Pleistocenic and Holocenic volcanic areas (Siebert et al., 2010) are also indicated. Plate boundaries were kept by Coffin et al. (1998).Earthquake precursors that occurred in the considered areas are shown in Fig. 2.

Fig. S.2. Images of earthquakes characterized by M>=5 (Bondar et al., 2015) that occurred in areas affected by relatively high heat flux (>=60 mW/m2) in the depth interval l0-20 km. Each seismic event is inserted in a pixel (100*100 km) indicating the local heat flux (Goutorbe et al., 2011). Pleistocenic and Holocenic volcanic areas (Siebert et al., 2010) are also indicated. Plate boundaries were kept by Coffin et al. (1998). Earthquake precursors that occurred in the considered areas are shown in Fig. 2.

Details about some geographic areas

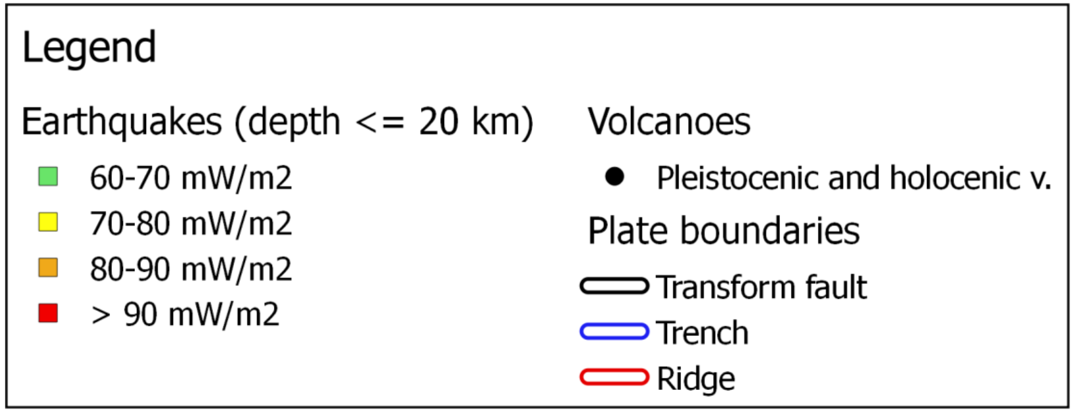

S2.a

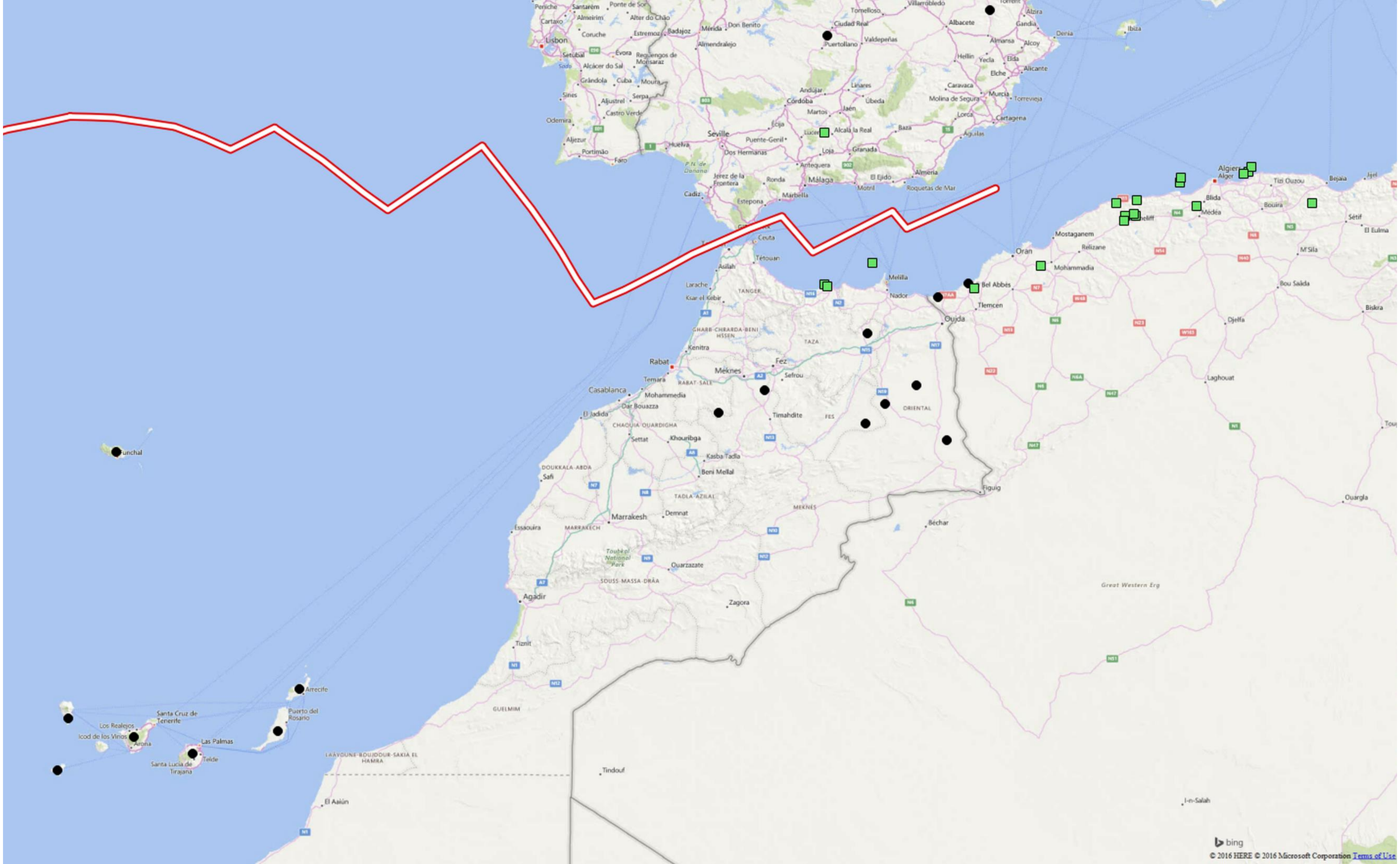

Lisbon
Setúbal
Évora
Badajoz
Mérida
Ciudad Real
Puertollano
Valdepeñas
Albacete
Almansa
Alcoy
Alicante
Denia
Ibiza
Elche
Murcia
Torrevieja
Cartagena
Lorca
Águilas
Caravaca
Córdoba
Jaén
Úbeda
Linares
Andújar
Seville
Dos Hermanas
Huelva
Faro
Portimão
Cadiz
Jerez de la Frontera
Ronda
Málaga
Marbella
Estepona
Granada
Loja
Antequera
Baza
Almería
El Ejido
Motril
Roquetas de Mar
Ceuta
Tétouan
Asilah
Larache
Ksar el Kebir
Melilla
Nador
Oujda
Tlemcen
Bel Abbès
Oran
Mostaganem
Relizane
Mohammadia
Algiers
Alger
Blida
Médéa
Bouira
Tizi Ouzou
Bejaia
Jijel
Sétif
El Eulma
M'Sila
Bou Saâda
Biskra
Djelfa
Laghouat
Ouargla
Rabat
Temara
Kenitra
Meknes
Fez
Sefrou
Taza
Casablanca
Mohammedia
Dar Bouazza
El Jadida
Settat
Khouribga
Kasba Tadla
Beni Mellal
Timahdite
Safi
Marrakesh
Demnat
Essaouira
Ouarzazate
Agadir
Zagora
Tiznit
Figuig
Béchar
Tindouf
El Aaiún
Great Western Erg
Funchal
Arrecife
Puerto del Rosario
Santa Cruz de Tenerife
Los Realejos
Icod de los Vinos
Arona
Las Palmas
Telde
Santa Lucía de Tirajana
I-n-Salah
bing
© 2016 HERE © 2016 Microsoft Corporation Terms of Use

S2.b

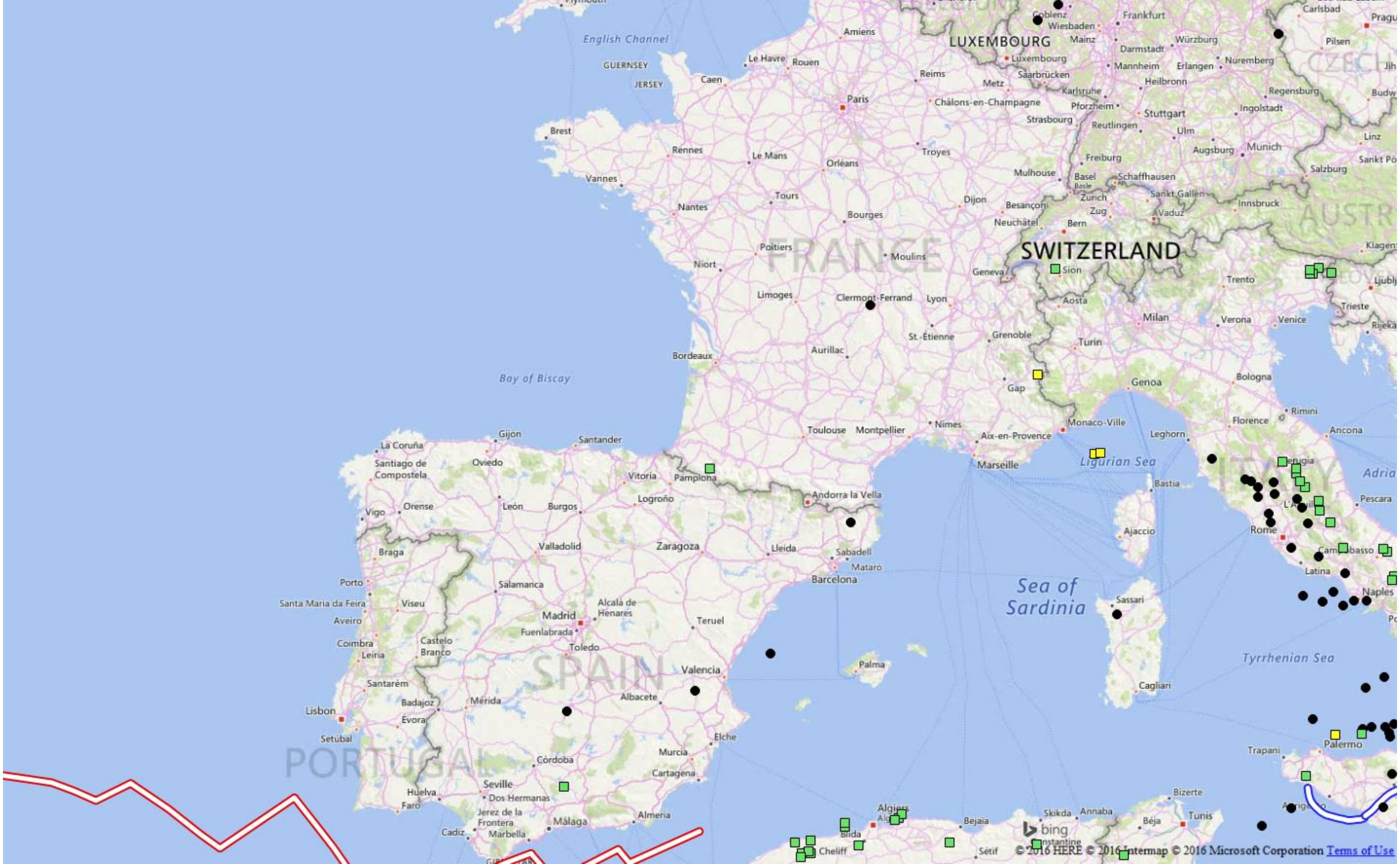
English Channel
GUERNSEY
JERSEY
LUXEMBOURG
Frankfurt
Wiesbaden
Mainz
Darmstadt
Würzburg
Nuremberg
Mannheim
Erlangen
Heilbronn
Karlsruhe
Pforzheim
Stuttgart
Reutlingen
Ulm
Augsburg
Munich
Ingolstadt
Regensburg
Carlsbad
Pilsen
Linz
Salzburg
Innsbruck
Freiburg
Basel
Schaffhausen
Zurich
Zug
Sankt Gallen
Vaduz
Bern
Neuchâtel
SWITZERLAND
Sion
Amiens
Le Havre
Rouen
Caen
Paris
Reims
Metz
Luxembourg
Saarbrücken
Châlons-en-Champagne
Strasbourg
Brest
Rennes
Le Mans
Orléans
Troyes
Vannes
Nantes
Tours
Dijon
Besançon
Mulhouse
Bourges
Poitiers
FRANCE
Moulins
Niort
Limoges
Clermont-Ferrand
Lyon
Geneva
Aosta
Trento
Verona
Venice
Trieste
Rijeka
Milan
St.-Étienne
Grenoble
Turin
Aurillac
Bordeaux
Bay of Biscay
Gap
Genoa
Bologna
Rimini
Florence
Ancona
Toulouse
Montpellier
Nîmes
Aix-en-Provence
Monaco-Ville
Leghorn
Marseille
Ligurian Sea
Bastia
Adria
Pescara
Rome
Ajaccio
Latina
Naples
Gijón
Santander
La Coruña
Santiago de Compostela
Oviedo
Vitoria
Pamplona
Logroño
Andorra la Vella
León
Burgos
Vigo
Orense
Braga
Valladolid
Zaragoza
Lleida
Sabadell
Mataró
Barcelona
Porto
Salamanca
Santa Maria da Feira
Viseu
Aveiro
Madrid
Alcalá de Henares
Fuenlabrada
Teruel
Coimbra
Leiria
Castelo Branco
Toledo
SPAIN
Valencia
Sea of Sardinia
Sassari
Palma
Tyrrhenian Sea
Santarém
Albacete
Cagliari
Lisbon
Badajoz
Mérida
Évora
Setúbal
Elche
PORTUGAL
Córdoba
Murcia
Cartagena
Trapani
Palermo
Seville
Huelva
Faro
Dos Hermanas
Jerez de la Frontera
Marbella
Cadiz
Málaga
Almeria
Algiers
Blida
Cheliff
Bejaia
Sétif
Skikda
Annaba
Bizerte
Tunis
Béja
bing
© 2016 HERE © 2016 Intermap © 2016 Microsoft Corporation Terms of Use

S2.c

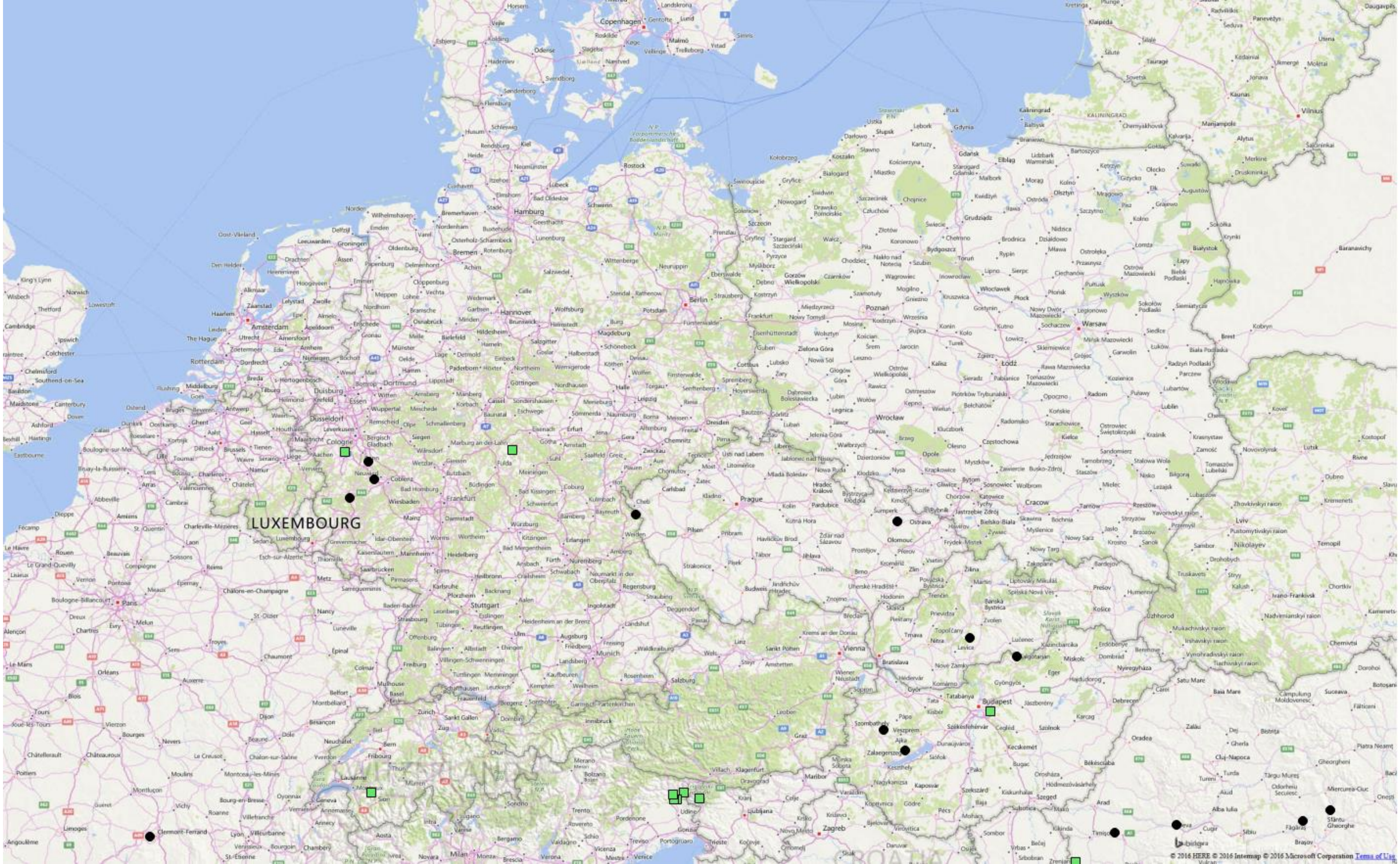
LUXEMBOURG
© 2016 HERE © 2016 Intermap © 2016 Microsoft Corporation Terms of Use

S2.d

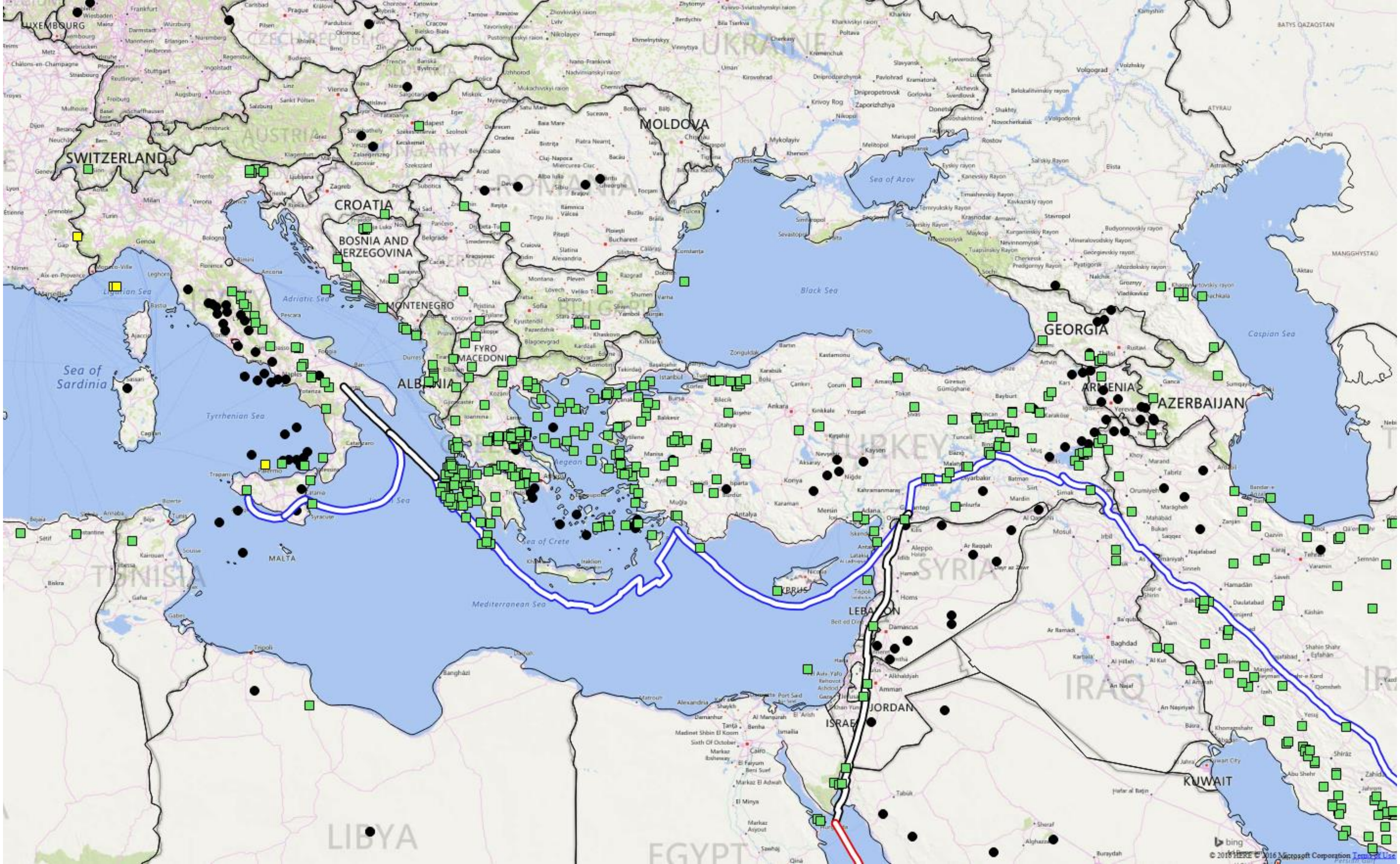
SWITZERLAND
AUSTRIA
CROATIA
BOSNIA AND HERZEGOVINA
MONTENEGRO
ALBANIA
FYRO MACEDONIA
ROMANIA
BULGARIA
MOLDOVA
UKRAINE
GEORGIA
ARMENIA
AZERBAIJAN
TURKEY
SYRIA
LEBANON
ISRAEL
JORDAN
IRAQ
KUWAIT
TUNISIA
LIBYA
EGYPT
MALTA
CYPRUS
Sea of Sardinia
Tyrrhenian Sea
Ligurian Sea
Adriatic Sea
Ionian Sea
Aegean Sea
Sea of Crete
Mediterranean Sea
Black Sea
Sea of Azov
Caspian Sea
bing
© 2016 HERE © 2016 Microsoft Corporation Terms of Use

S2.e

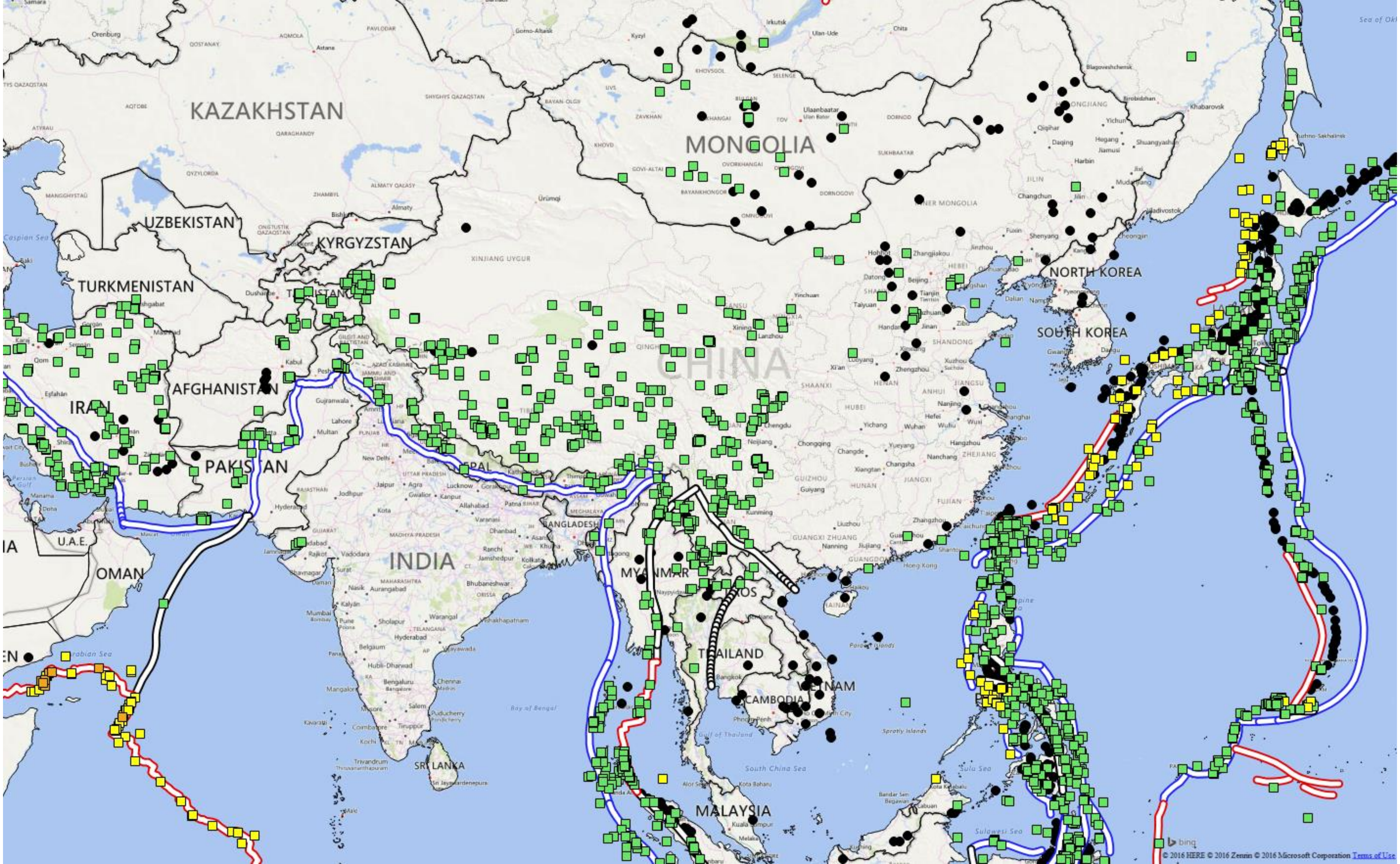
KAZAKHSTAN
MONGOLIA
UZBEKISTAN
KYRGYZSTAN
TURKMENISTAN
AFGHANISTAN
IRAN
PAKISTAN
CHINA
NORTH KOREA
SOUTH KOREA
INDIA
OMAN
U.A.E.
MYANMAR
THAILAND
CAMBODIA
VIETNAM
MALAYSIA
SRI LANKA
© 2016 HERE © 2016 Zenrin © 2016 Microsoft Corporation Terms of Use

S2.f

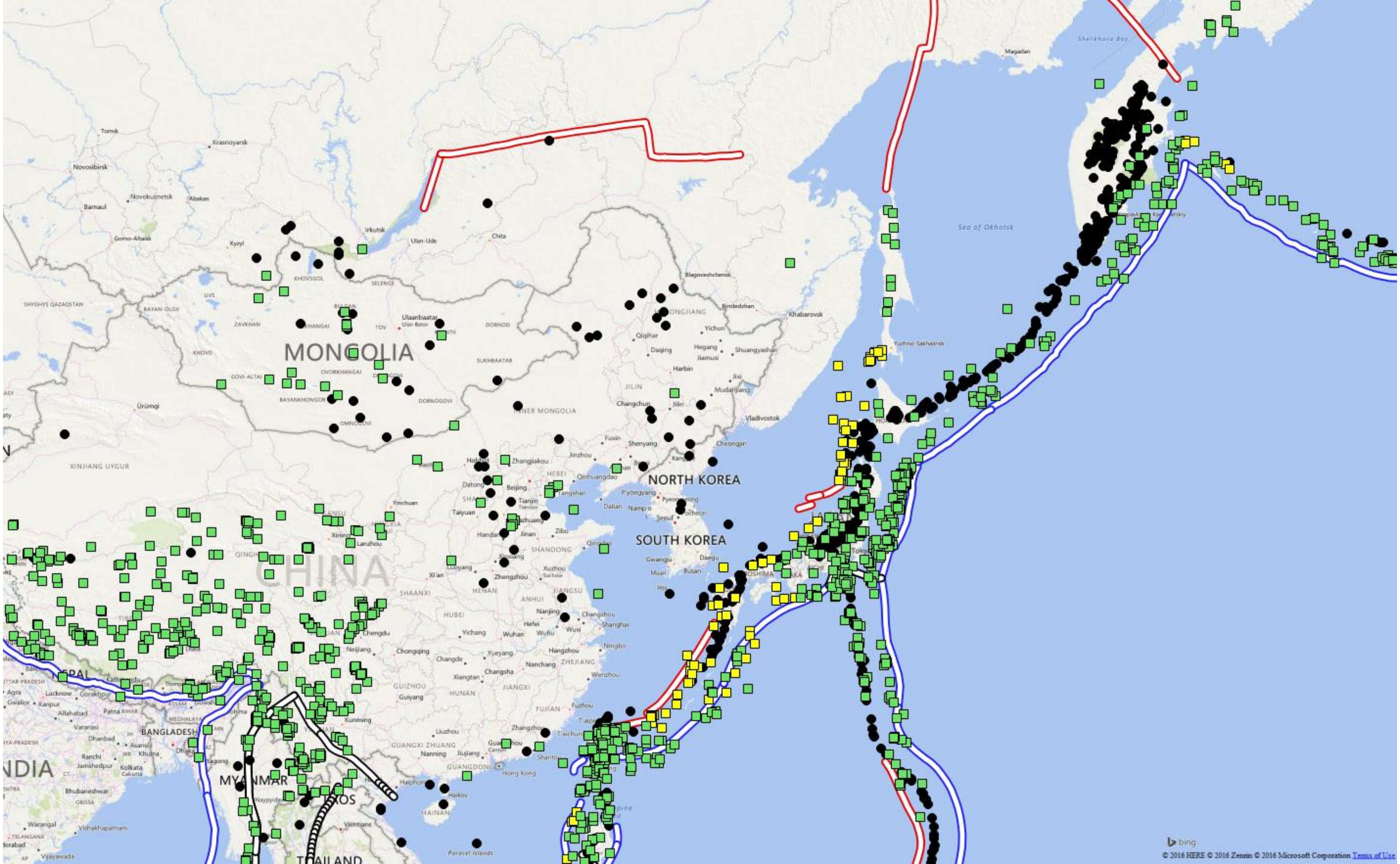
MONGOLIA
CHINA
NORTH KOREA
SOUTH KOREA
MYANMAR
INDIA
BANGLADESH
THAILAND
Sea of Okhotsk
© 2016 HERE © 2016 Zenrin © 2016 Microsoft Corporation Terms of Use

S2.g

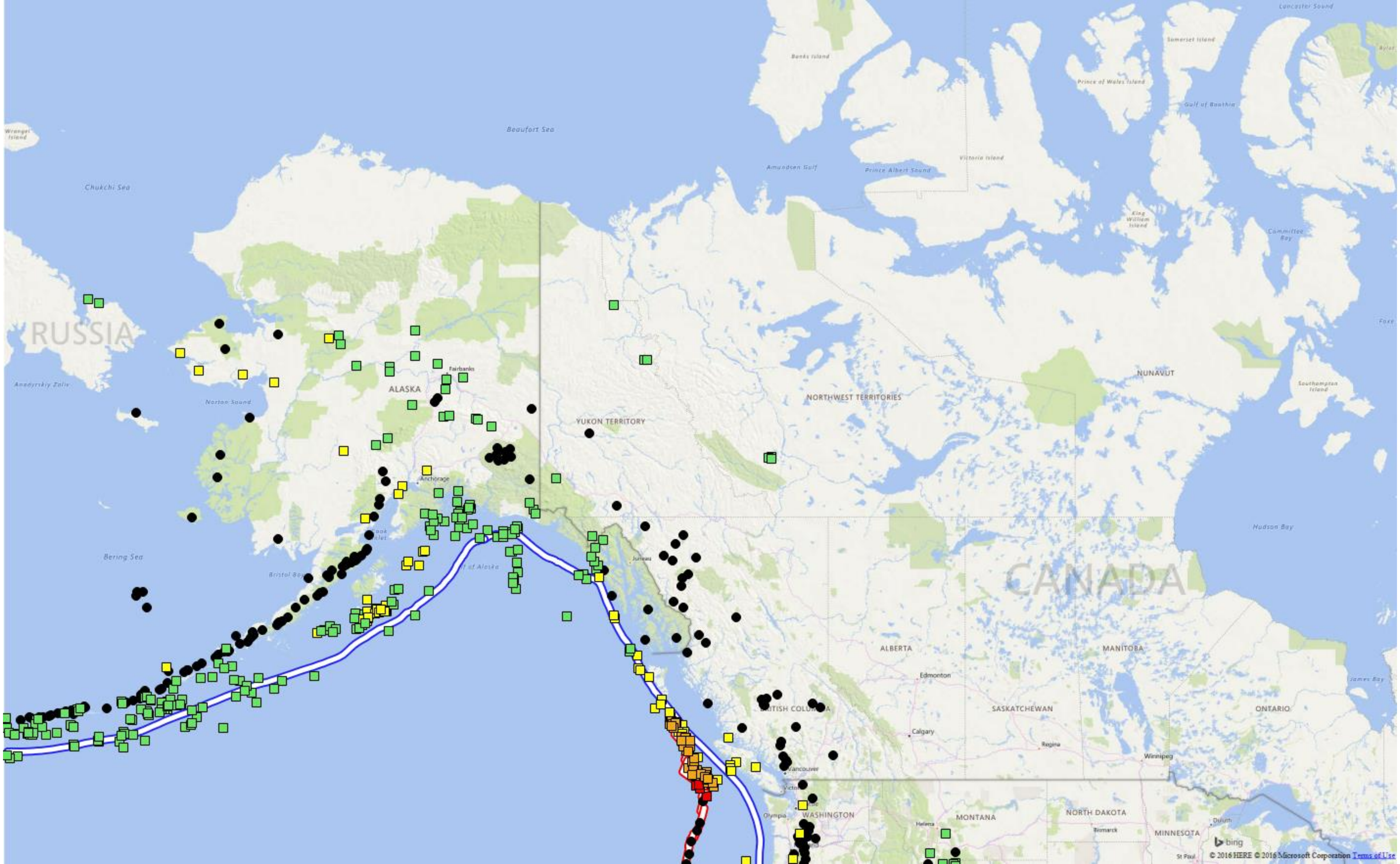
Beaufort Sea
Chukchi Sea
RUSSIA
ALASKA
Fairbanks
Anchorage
Norton Sound
Bering Sea
Bristol Bay
Juneau
YUKON TERRITORY
NORTHWEST TERRITORIES
NUNAVUT
CANADA
BRITISH COLUMBIA
ALBERTA
SASKATCHEWAN
MANITOBA
ONTARIO
Edmonton
Calgary
Regina
Winnipeg
Vancouver
Victoria
Olympia
WASHINGTON
MONTANA
NORTH DAKOTA
MINNESOTA
Helena
Bismarck
Duluth
St Paul
Hudson Bay
James Bay
Banks Island
Victoria Island
Amundsen Gulf
Prince Albert Sound
Prince of Wales Island
Somerset Island
Gulf of Boothia
King William Island
Committee Bay
Southampton Island
Lancaster Sound
Wrangel Island
Anadyrskiy Zaliv
Gulf of Alaska
bing
© 2016 HERE © 2016 Microsoft Corporation Terms of Use

S2.h

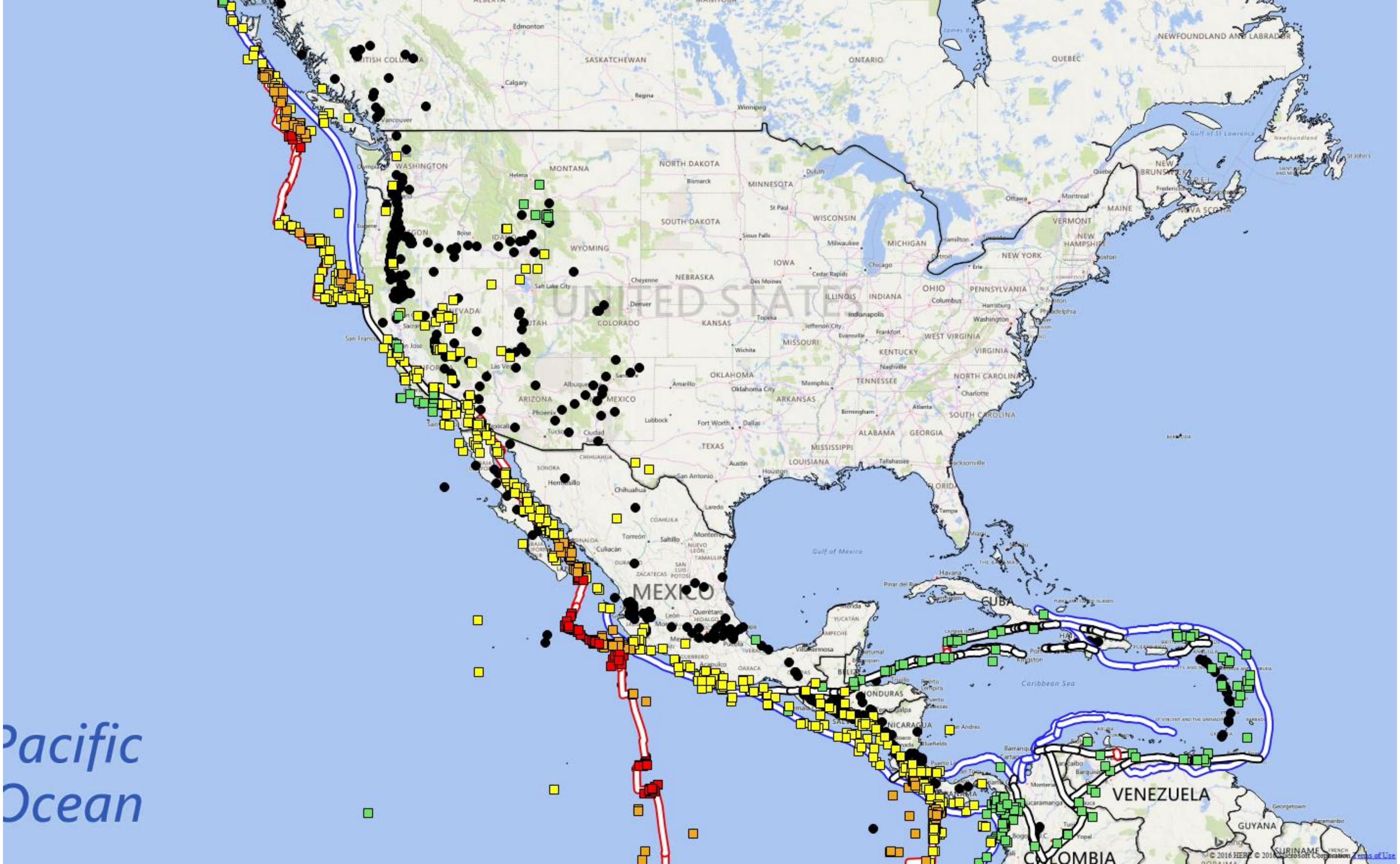

BRITISH COLUMBIA
SASKATCHEWAN
ONTARIO
QUEBEC
NEWFOUNDLAND AND LABRADOR
Edmonton
Calgary
Regina
Winnipeg
Vancouver
WASHINGTON
MONTANA
NORTH DAKOTA
MINNESOTA
SOUTH DAKOTA
WISCONSIN
MICHIGAN
WYOMING
IOWA
NEBRASKA
UNITED STATES
NEVADA
UTAH
COLORADO
KANSAS
MISSOURI
ILLINOIS
INDIANA
OHIO
PENNSYLVANIA
NEW YORK
VERMONT
NEW HAMPSHIRE
MAINE
NEW BRUNSWICK
NOVA SCOTIA
WEST VIRGINIA
VIRGINIA
KENTUCKY
TENNESSEE
NORTH CAROLINA
SOUTH CAROLINA
GEORGIA
ALABAMA
MISSISSIPPI
LOUISIANA
ARKANSAS
OKLAHOMA
TEXAS
ARIZONA
NEW MEXICO
FLORIDA
Gulf of Mexico
MEXICO
CUBA
Caribbean Sea
HONDURAS
NICARAGUA
VENEZUELA
COLOMBIA
GUYANA
SURINAME
Pacific
Ocean
© 2016 HERE © 2016 Microsoft Corporation Terms of Use

S2.i

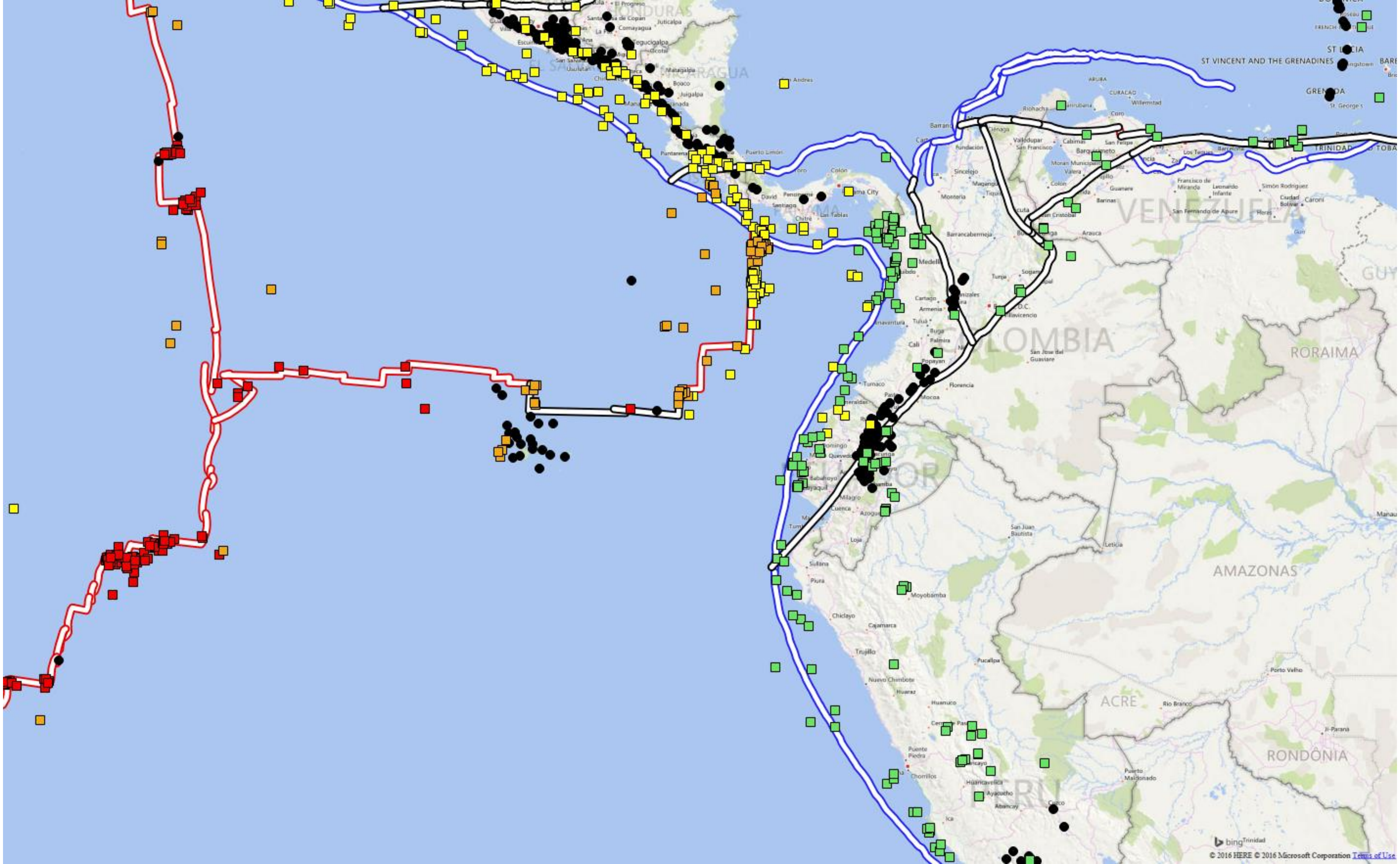
ST VINCENT AND THE GRENADINES
VENEZUELA
RORAIMA
AMAZONAS
ACRE
RONDÔNIA
© 2016 HERE © 2016 Microsoft Corporation Terms of Use

S2.j

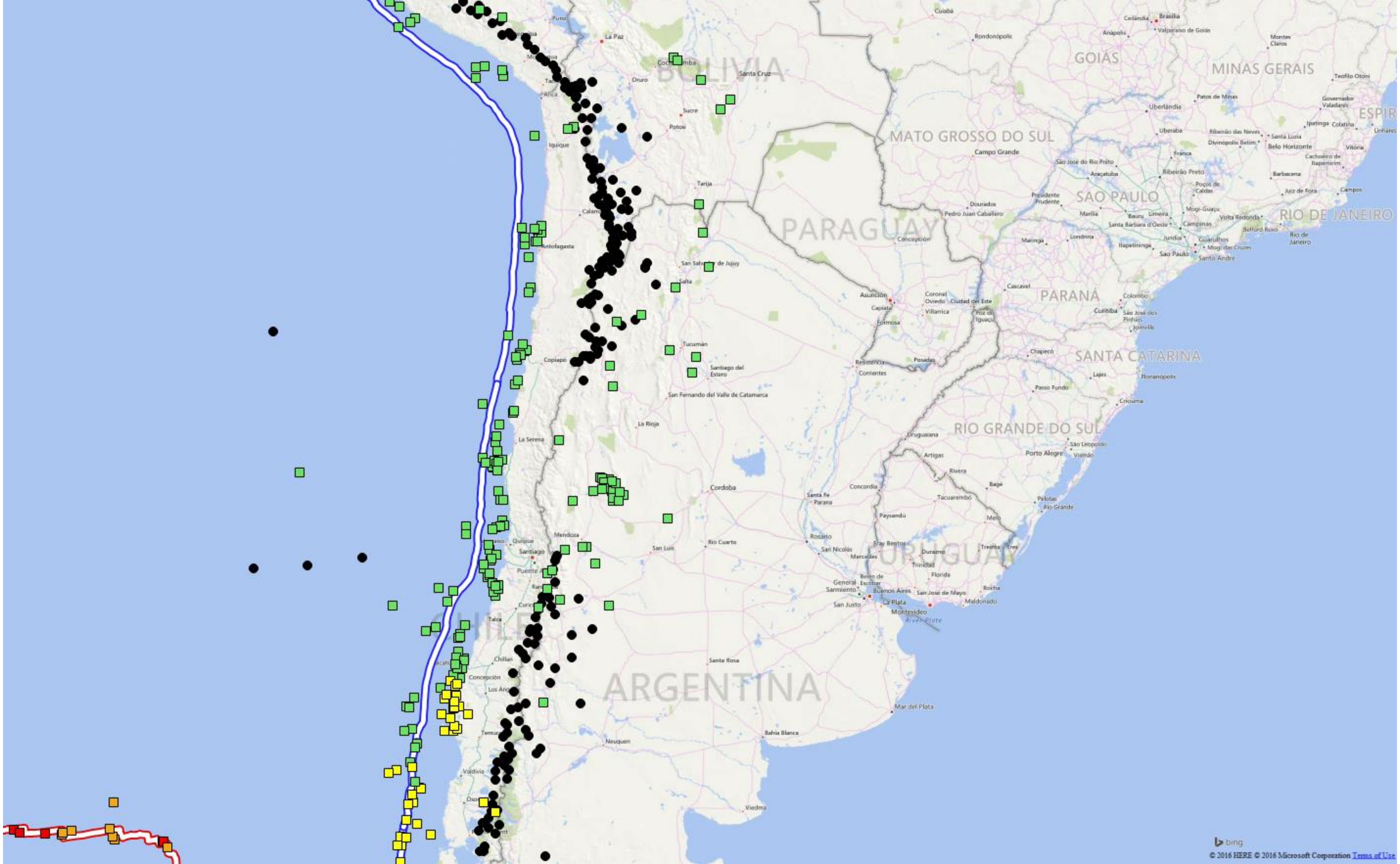
BOLIVIA
PARAGUAY
ARGENTINA
URUGUAY
CHILE
MATO GROSSO DO SUL
GOIÁS
MINAS GERAIS
SAO PAULO
RIO DE JANEIRO
PARANÁ
SANTA CATARINA
RIO GRANDE DO SUL
La Paz
Santa Cruz
Sucre
Potosí
Tarija
Antofagasta
Copiapo
La Serena
Santiago
Mendoza
Cordoba
Rosario
Buenos Aires
Montevideo
Asunción
Concepción
Valdivia
Neuquen
Bahía Blanca
Mar del Plata
Santa Rosa
Viedma
La Rioja
Tucumán
Salta
Curitiba
Porto Alegre
Campo Grande
Brasília
bing
© 2016 HERE © 2016 Microsoft Corporation Terms of Use

S2.k

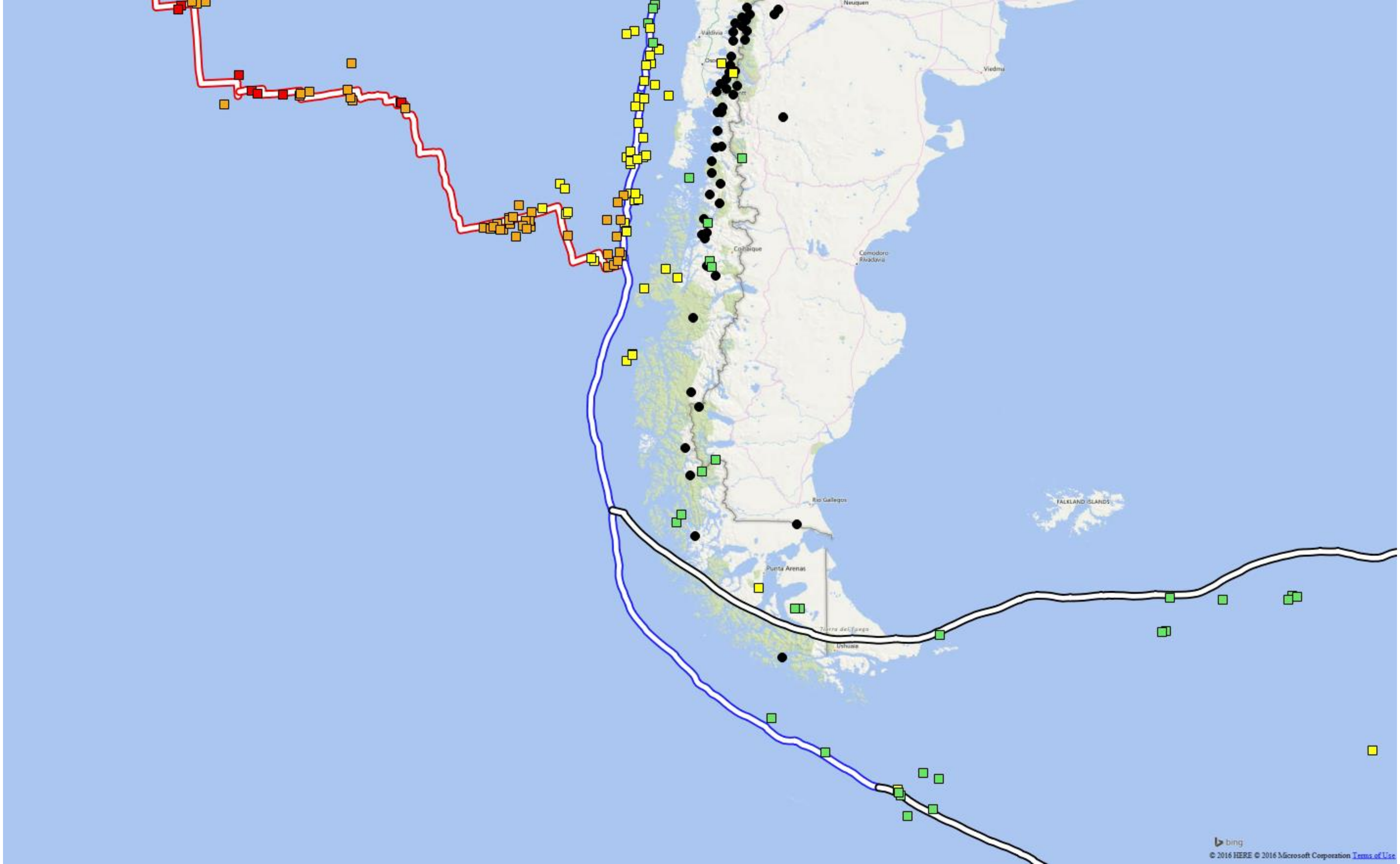

Neuquen
Valdivia
Viedma
Coihaique
Comodoro Rivadavia
Rio Gallegos
FALKLAND ISLANDS
Punta Arenas
Tierra del Fuego
Ushuaia
bing
© 2016 HERE © 2016 Microsoft Corporation Terms of Use

S2.I

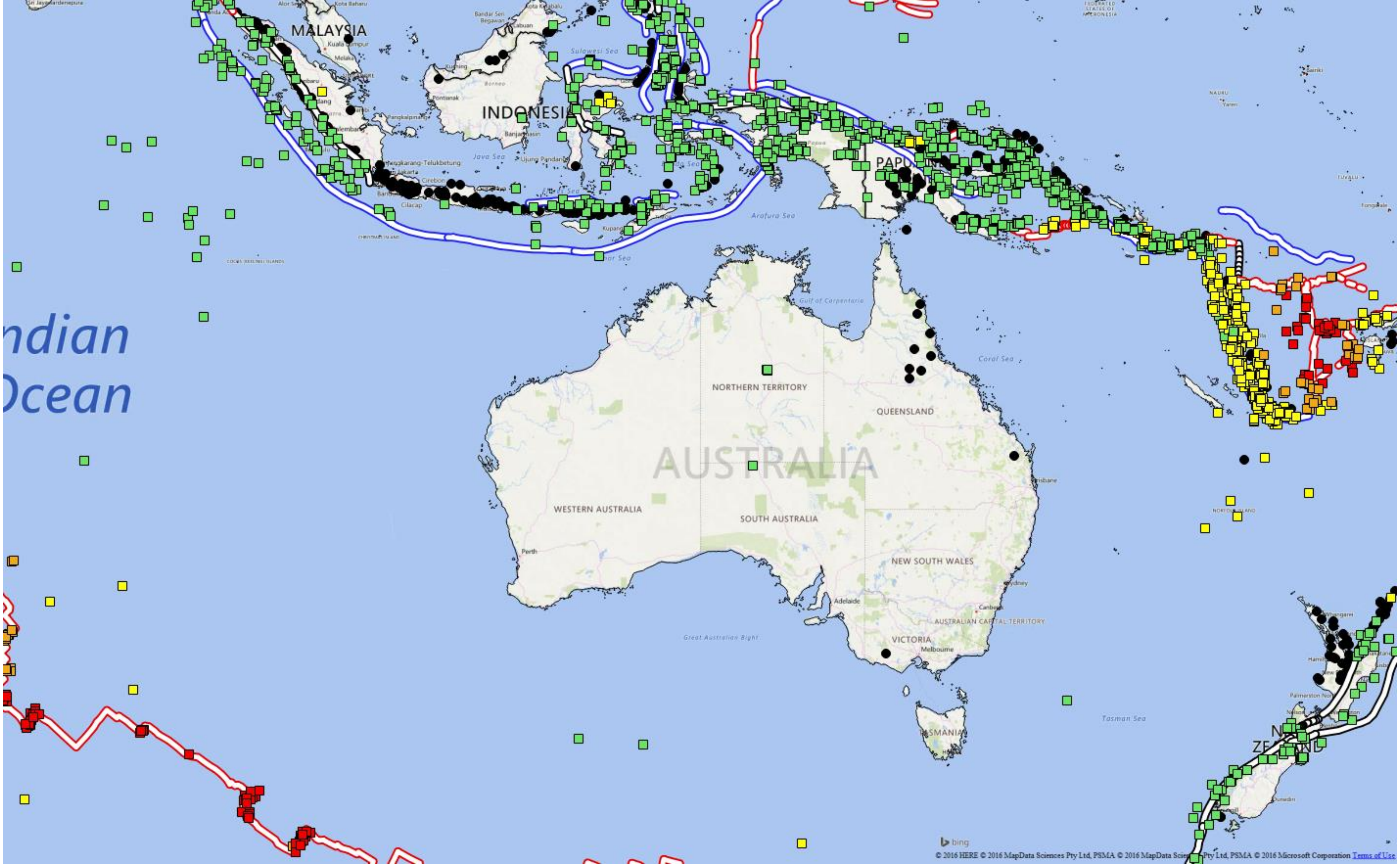

MALAYSIA
INDONESIA
Indian
Ocean
AUSTRALIA
NORTHERN TERRITORY
QUEENSLAND
WESTERN AUSTRALIA
SOUTH AUSTRALIA
NEW SOUTH WALES
VICTORIA
TASMANIA
Coral Sea
Tasman Sea
Arafura Sea
Java Sea
Sulawesi Sea
Gulf of Carpentaria
Great Australian Bight
Perth
Adelaide
Melbourne
Sydney
Brisbane
bing
© 2016 HERE © 2016 MapData Sciences Pty Ltd, PSMA © 2016 MapData Sciences Pty Ltd, PSMA © 2016 Microsoft Corporation Terms of Use

S2.m

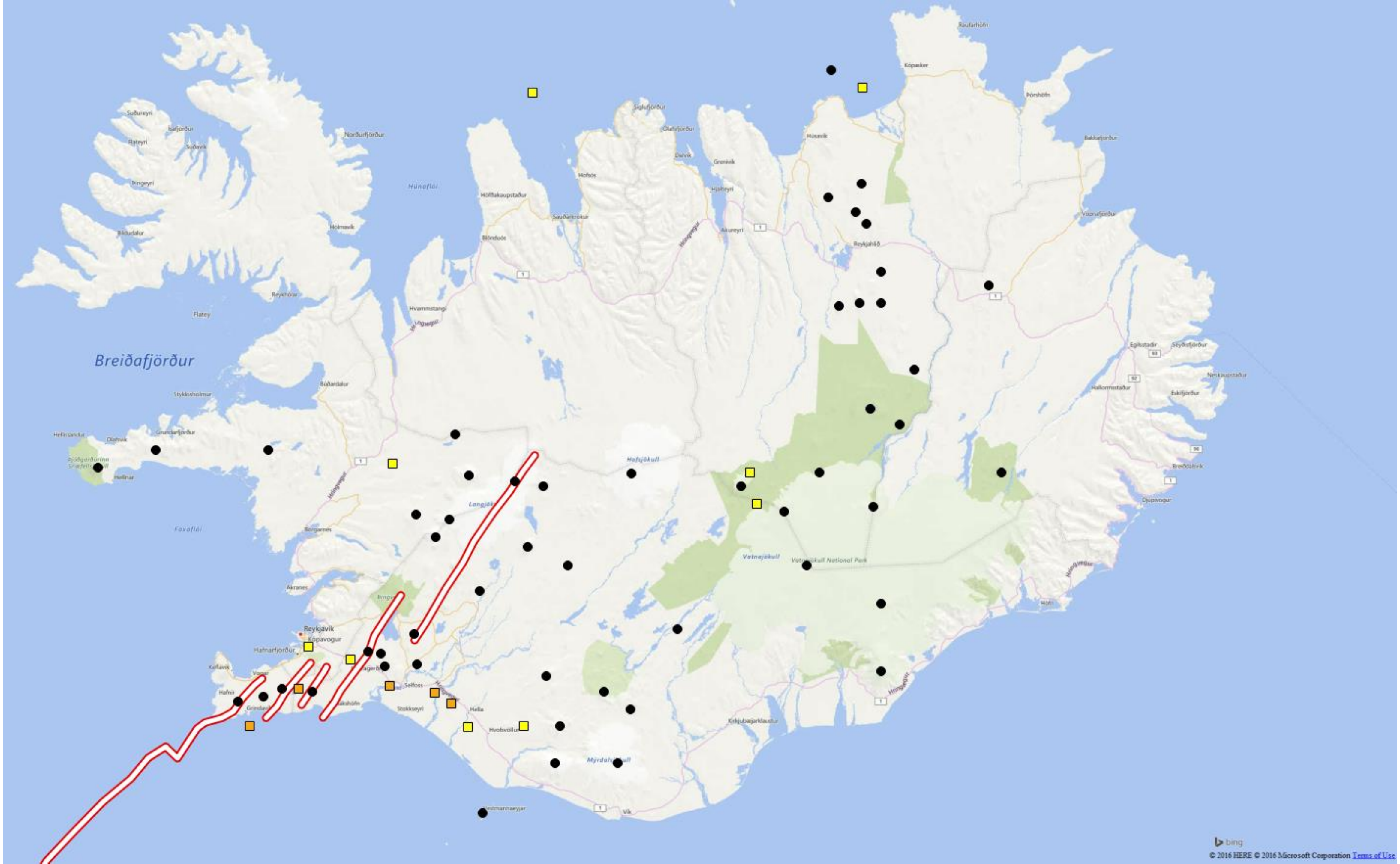
Breiðafjörður
Reykjavík
Kópavogur
Hafnarfjörður
Selfoss
Hella
Vík
Akureyri
Húsavík
Egilsstaðir
Hofsjökull
Langjökull
Vatnajökull
Vatnajökull National Park
Mýrdalsjökull
bing
© 2016 HERE © 2016 Microsoft Corporation Terms of Use

S2.n

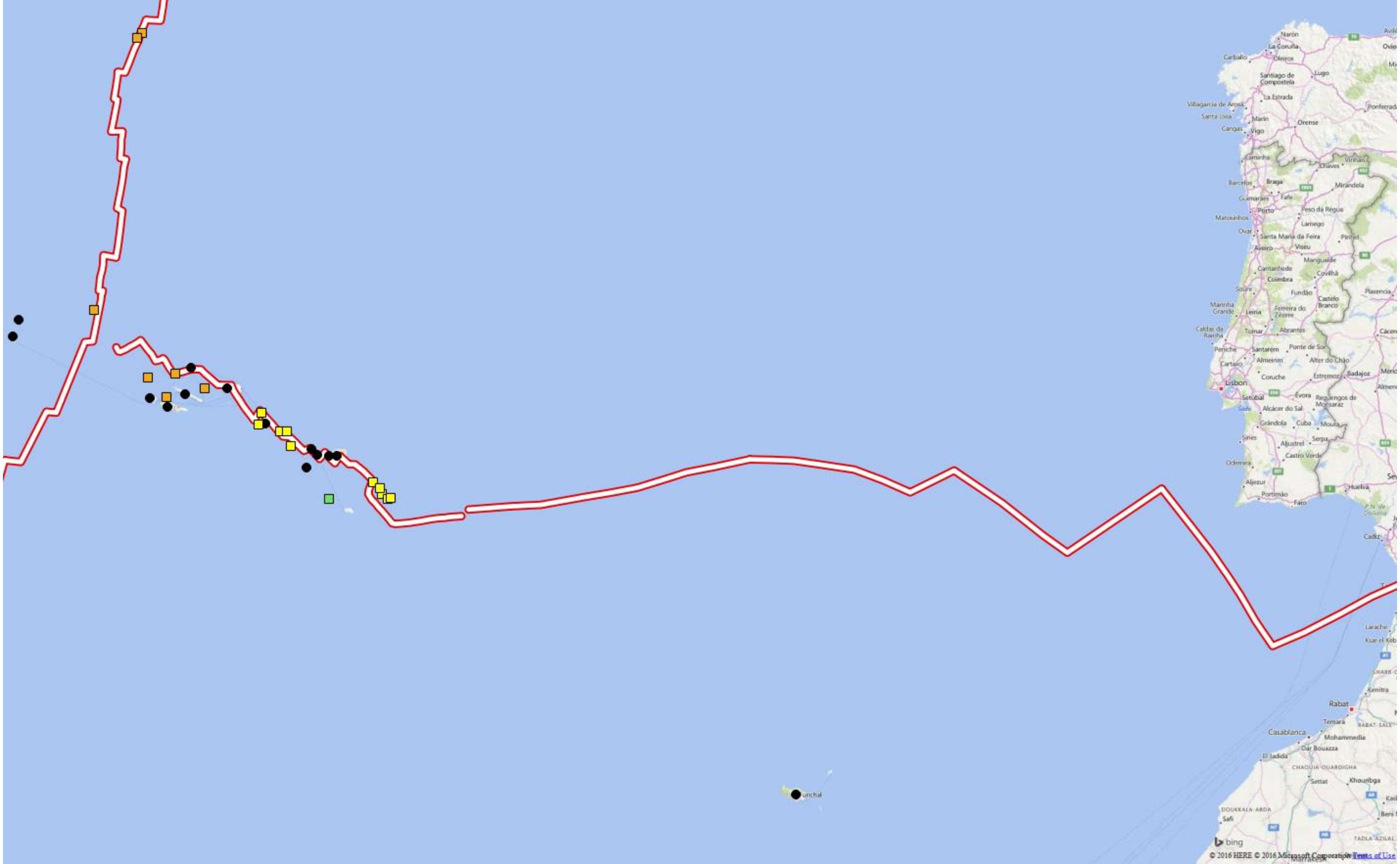
Lisbon
Porto
Coimbra
Rabat
Casablanca
Funchal
bing
© 2016 HERE © 2016 Microsoft Corporation Terms of Use

Figure S_3

Prince B.B.Galitzin in 1911 proposed a research programme to forecast earthquakes (Zarkov, 1986). This programme was reprinted in 1960 (Galitzin, 1960) and included the study of following topics:

1. the frequency, magnitude and waveform of recorded seismic waves;
2. the velocity of propagation of seismic waves to evaluate the state of stress;
3. geodetic measurements to identify slow crustal deformations;
4. gravimetric measurements;
5. chemical and physical parameters in the waters of springs and of wells

№	In Russian	In English
1	Химические анализы воды различных минеральных источников, а также анализ содержащихся в воде и выделяющихся из нее газов. Эти анализы должны быть распространены на редкие элементы.	Chemical analysis of waters and gases of mineral springs. These analysis should include rare elements.
2	Повторение этих детальных анализов каждые 3-5 лет или чаще, если какой-нибудь контрольный анализ покажет изменение состава какого-либо из этих минеральных источников.	Mineral springs every 3-5 years or more frequently if a parameter changes.
3	Систематический еженедельный контрольный анализ одного источника каждого типа, а именно, определение двух главных составных частей его. Такие упрощенные анализы должны проводиться для всех источников один раз в три месяца, например, 1 января, 1 апреля, 1 июня и 1 октября.	Weekly control of two main parameters in waters of mineral springs. A more detailed analysis should be carried out every three months, for example, January 1, April 1, June 1 and October 1.
4	Автоматическая непрерывная регистрация дебита источников.	Automatic continuous recording of the water flow rate of springs.
5	Регистрация колебаний уровня источников при помощи лимниграфов, если технические условия это позволяют.	Registration of water level fluctuations in wells if the technical conditions allow it.
6	Систематическая регистрация температуры источников на определенной глубине под земной поверхностью при помощи электрических термографов. Ежедневное одноразовое контрольное определение этой же температуры ртутным термометром.	Systematic recording of underground temperature by electrical thermography. Daily calibration of the equipment by a mercury thermometer.
7	Исследование физических свойств источника в определенные интервалы времени: радиоактивность, проводимость, осмотическое давление и т.д.	Recording of some physical parameters of waters in mineral springs: radioactivity, electric conductivity, osmotic pressure, etc.
8	Исследование физических свойств осадков источников, выделяющихся из них газов, а также горных пород, находящихся вблизи источников.	Study of the physical properties of geological formations affected by gas emissions,
9	Систематическое исследование количества (массы) выделяющихся газов.	Monitoring of the flow rate in gas emissions.
10	Наблюдения над интермитенцией источников с помощью саморегистрирующих приборов.	Observations on intermittent springs (such as geysers).
11	Наблюдения за температурой слоев Земли на различных глубинах.	Monitoring of the temperature of the Earth at different depths.
12	Зависимость вышеназванных факторов от метеорологических и сейсмических явлений.	Study of the influence of meteorological parameters and of seismic events on observed data

Table S.1. Catalogue of historical earthquakes of Italy characterized by M>=5.5 reviewed by Boschi et al. (1995). The Catalogue lists geochemical variations in waters, variations in the water flow rate, variations in gas emissions, anomalous behaviour of animals, light and electromagnetic phenomena, ground deformations and eventual other effects such as sounds or thunder. The literature sources are reported in the text. Some of reported effects were observed before the mainshock in Ischia Island (southern Italy) in 1881 and in 1883. The earthquake that occurred in 1881 (Rovida et al., 2011) is not listed in Boschi et al. (1995) due to M being slightly <5.5 and was studied, among others, by De Rossi (1884) and by Molin et al. (2003). In 1881 and 1883, geochemical and hydrogeologic precursory phenomena were observed. In 1883, fluid-related precursory phenomena were observed jointly with ground deformation precursory phenomena. The Irpinia earthquake in 1980 was studied by Balderer and Martinelli (1995, §). The 1968 earthquake was also studied by Dall'Aglio (1976).

								PRESEISMIC						COSEISMIC - POSTSEISMIC						Reference (pag. / ID)						
ID	YEAR	MONTH	DAY	PLACE	Latitude N	Longitude E	N° of event	Variations in waters geochem. parameters	Variations in geseous emissions	Flow rate variations	Animals behaviour	Light and Electrom. phenomena	Others	Variations in waters geochem. parameters	Variations in geseous emissions	Flow rate variations	Animals behaviour	Light and Electrom. phenomena	Others	(#) Baratta, 1901	(*) Mercalli, 1883	(+) Bonito, 1691	(^) Boschi et al., 1995	(ç) De Rossi, 1884	($) Balderer and Martinelli, 1995	($) Dall'Aglio, 1976
1	1117	1	3	Veronese	45°48'	10°54'	35							2 #*		1 *				24	284					
2	1169	2	4	Mar Ionio	37°30'	15°20'	62							2 #*		2 #*			2 *	27	282					
3	1198			Pozzuoli	40°49'	14°10'	79												1 #	29-30						
4	1222	12	25	Bresciano	45°32'	10°12'	89									1 *			1 *		285					
5	1230	4	5	Villa S. Giovanni	38°15'	15°40'	99												1 *		345					
6	1231	6	1	Montecassino	41°29'	13°49'	100							2 #						33			12310601			
7	1293	7	11	Pistoia	43°55'	10°55'	160												1 #	41						
8	1320	5	28	Commenda	42°30'	12°0'	202												2 *		223					
9	1329	6	28	M. Etna Nord	37°50'	15°0'	216									2 #			2 #	48						
10	1348	1	25	Tarvisio	46°35'	13°40'	233									2 #*			2 ^	51	286-287		13480125			
11	1352	12	25	Monterchi	43°30'	12°10'	244												1 +			572-573				
12	1456	12	5	Napoletano	41°31'	14°31'	413								2 +	2 #+			2 +	74	602					
13	1501	6	5	Vignola	44°30'	10°56'	501							2 #		2 #			1 #	84-85						
14	1502			Rieti	42°23'	12°57'	510							2 #						85						
15	1511	3	26	Friuli	46°15'	13°20'	541									1 #			1 #	88-89						
16	1514	7	12	Gemona	46°17'	13°9'	594												1 #	90						
17	1538	9	26	Pozzuoli	40°50'	14°10'	679							2 +	2 +				2 +			617-678-680-681				
18	1542	12	10	Siracusano	37°10'	15°10'	694							2 #+						97	290	688				
19	1545	6	9	Borgo Val di Taro	44°28'	9°47'	697									2 #				634						
20	1550	2	28	Castelletto	44°25'	7°35'	709									1 #			2 +	635		692				
21	1558	4	13	M. Sante Marie	43°20'	11°30'	718									2 #				100						
22	1561	8	19	Vallo di Diano	40°20'	15°35'	725									2 #		1 +		102		698				
23	1564	7		Medio Tirreno	40°45'	14°10'	736												2 +			702				
24	1564	7	20	La Bollene	44°0'	7°17'	738								1 #	1 #			1 #	104						
25	1570	11	17	Ferrara Sud	44°50'	11°39'	755							1 #		1 #		1 #	1 #*	106	291					
26	1594			Ferrara sud	44°50'	11°40'	825							1 *							348					
27	1600	9		Issime	45°40'	7°50'	845									2 #				637						
28	1611	9	8	Borgo S. Lorenzo	44°0'	11°20'	866									1 #				114						
29	1613	8	25	Naso	38°5'	14°45'	870							2 *	2*				1 *#	115	291					
30	1618	9	4	Sondrio	46°15'	10°0'	881									1 +	1 +					747				
31	1624	3	18	Ferrara Sud	44°50'	11°39'	904									1 #			1 #+	119		749				
32	1624	10	3	Mineo	37°20'	14°45'	909												2 #	119						
33	1626	3	27	Squillace	38°50'	16°30'	919								2 *				2 *		291					
34	1627	7	30	Capitanata Sett.	41°47'	15°18'	928							1 #		1 #*+			1 #*+	121-123-124	292	753-754				
35	1627	9	6	Capitanata Sett.	41°41'	15°23'	935												2 *		292					
36	1631	12	15	Vesuvio	40°50'	14°25'	938							1 *		1 *			1 +		228	762				
37	1638	1	18	Calabria	39°0'	16°15'	952							2 +	2 +				2 +			766-767-768				
38	1638	3	27	Calabria	39°0'	16°15'	953									2 ^			1 ^				16380327			
39	1646	4	5	Mar Ligure	43°30'	10°5'	991												1 #	135						
40	1661	3	22	Civitella di Romagna	44°2'	11°54'	1026								2 +				1 +			788				
41	1672	4	14	Rimini	44°5'	12°40'	1056											1 *	1 #	147-150	331					
42	1688	6	5	Campania	41°19'	14°34'	1108							1 ^*		1 #			2 #^	162	294-348		16880605			
43	1690	12	23	Ancona	43°37'	13°30'	1124								2 +				2 +			808				
44	1691			M. Gibliscemi	37°15'	14°15'	1132												1 #	164						

45	1692	2	27	Pignataro	41°29'	13°48'	1134											2	#	165		
46	1693	1	9	Brucoli	37°20'	15°10'	1143	2	# 1*	1	*	2	#*			1	*	1	#*	165-169	295-296	
47	1694	9	8	Basilicata	40°52'	15°26'	1166			1	#*	1	#					1	#	179-181		
48	1703	1	14	Norcia	42°40'	13°10'	1284	1	*	1	*	1	*	1	*			1	#*	189-197	298	
49	1717	4	22	Castroreale	38°10'	15°15'	1415											1	#	206		
50	1717	6	27	Catania Sud	37°30'	15°0'	1419											1	*		345	
51	1727	5	8	Canale di Sicilia	37°30'	13°0'	1570	2	#									1	#	213		
52	1728	2	8	Teano	41°17'	13°59'	1631											1	#	214		
53	1729	6	23	Firenze	43°50'	11°15'	1644									1	#			215		
54	1731	3	20	Foggia	41°28'	15°33'	1667					1	#			1	*	1	^	217	299	17310320
55	1732	11	29	Irpinia	41°5'	15°7'	1726					1	^							220		17321129
56	1738	11	6	Parma Ovest	44°50'	10°15'	1768									1	#			226		
57	1739	5	10	Gioiosa Marea	38°10'	14°50'	1776	2	#*			2	#*					1	^*	227	300	17390510
58	1742	1	16	Livorno	43°32'	10°15'	1804					1	*	1	*			1	#*	231	300	
59	1750	11	28	Pordenone	45°57'	12°42'	1982											1	*		345	
60	1753	3	9	Massello	45°0'	7°0'	2041											1	#	242		
61	1755	12	9	Chambery (Svizzera)	46°15'	8°0'	2066											1	#	644		
62	1756	4	13	Treviso Nord	45°40'	12°15'	2079											1	#	244		
63	1756	8	17	Padova	42°25'	11°50'	2085											1	#	244		
64	1771	1	28	Alba	44°40'	8°0'	2231											1	#	253		
65	1774	3	4	Sala Baganza	44°45'	10°15'	2297											1	#*	255	345	
66	1777	10	5	Radicofani	42°52'	11°43'	2359											1	#	256		
67	1779	6	1	Fontanelice	44°20'	11°30'	2374	1	#*	2	*	1	*					1	#*	258-259	303-345	
68	1779	8	8	Medio Tirreno	40°45'	14°15'	2403					2	*								236	
69	1780	2	6	Fontanelice	44°20'	11°30'	2457											1	*		345	
70	1781	1	3	Siena	43°20'	11°20'	2494			2	*			2	*			1	*#	261	303	
71	1781	4	4	Castrocaro	44°14'	11°50'	2502			2	^	2	^					1	^			17810404
72	1781	6	3	Cagli	43°34'	12°37'	2525	1	#*			1	#*	1	*	1	*	1	#*	265-266	303-304	
73	1783	2	5	Calabria	38°20'	16°0'	2700	1	*	1	^	1	*^	1	#*	1	*	1	*^	269	304-307-308	17830205
74	1784	6	7	Villa S. Giovanni	38°15'	15°42'	4009											1	*		345	
75	1785	10	2	Labro	42°32'	12°45'	4259	2	*	2	*							1	#	295	237	17851009
76	1786	12	25	Riccione Marina	44°0'	12°36'	4475									1	*	1	#	299	331	
77	1789	9	30	Città di Castello	43°37'	12°14'	4589	1	#			1	#^					1	#	303		17890930
78	1790	5		Niscemi	37°9'	14°24'	4601													648		
79	1791	10	11	Calabria	38°44'	16°9'	4614											1	#	305		
80	1794	6	7	Tramonti di Sotto	46°18'	12°46'	4681											1	#	307		
81	1796	10	22	Medicina	44°30'	11°35'	4747											1	#	310		
82	1798	5	26	Siena	43°20'	11°20'	4761											1	*#	310	310	
83	1802	5	12	Offanengo	45°23'	9°49'	4844	1	*	1	*	1	*	1	*			1	#*	314	239-311	
84	1804	10	18	Tegoia	43°20'	11°5'	4861	1	*												348	
85	1805	7	26	Baranello	41°32'	14°31'	4869	1	#*	1	*	1	#*	1	#*	1	#*	1	#*	318-322-323	311-367	
86	1806	2	12	Correggio	44°50'	10°45'	4888									1	#	1	#	324		
87	1806	8	26	Velletri	41°43'	12°44'	4919											2	*		239	
88	1808	4	2	Bobbio	44°50'	7°12'	4945	1	^	1	#	1	^			1	*	1	#*	329	312-345	18080402
89	1809	2	4	Bobbio	44°50'	7°12'	5072											1	*		345	
90	1809	8	14	Lucoli	42°20'	13°25'	5084	2	#									1	#	330		
91	1810	12	25	Correggio	44°50'	10°45'	5101											1	*		345	
92	1812	9	11	Romola	43°45'	11°5'	5136											1	*		345	
93	1817	1	14	Macauda	37°30'	13°5'	5191	1	#			2	*					1	#*	337	312-313	
94	1818	2	20	Catanese	37°36'	15°6'	5222	1	*			1	*	1	#*	1	*	1	#*^	338-339	313-241	18180220
95	1818	9	8	Madonie	37°50'	14°0'	5246											1	#	344	313	
96	1821	3	22	Rieti	42°25'	12°50'	5288											1	#	347		
97	1823	3	5	Naso	38°7'	14°47'	5335	1	#*			1	#*					1	#*	350	314	
98	1824	8	12	Pieve S. Stefano	43°45'	12°0'	5375			2	*							2	*		242	
99	1826	2	1	Tito	40°35'	15°40'	5396	1	* 2#					1	*	1	*	1	#*	353	314-348	
100	1826	11	11	Pavia	45°10'	9°10'	5422											1	#	355		
101	1827	8	14	Palermo	38°7'	13°21'	5441									1	#	1	#	355		
102	1828	2	2	Casamicciola	40°45'	13°45'	5460	2	^									1	#	356		18280202
103	1828	4	8	Alto Adriatico	44°10'	12°30'	5472											1	#	357		
104	1828	10	9	Varzi	44°50'	9°10'	5491											2	#	360		
105	1828	1		Albano	41°44'	12°39'	5517			1	*			1	*	1	*	1	*		315	

106	1831	5	26	Taggia	43°50'	7°50'	5824	2	^	1	*	1	^					1	#*^	364	317-318	18310526
107	1831	6	28	Macauda	37°30'	13°5'	5838													365		
108	1831	9	11	Castelnovo	44°50'	10°30'	5874	1	*			2	*	1	*	1	*	1	*		318-348	
109	1831	10	27	Spello	42°56'	12°42'	5881					1	#*			1	*	1	#*	368-369	316	
110	1832	3	8	Cotronese	39°10'	16°49'	5906	1	*			1	^	1	*	1	*	1	#*	370	317-348	18320308
111	1832	9	10	Castelnovo	44°46'	10°30'	5975			2	*										245	
112	1835	2	6	Borgo S. Lorenzo	43°56'	11°23'	6038											1	#	376		
113	1835	10	12	Castiglione	39°22'	16°15'	6063									1	#*			377	318	
114	1836	4	24	Rossano	39°36'	16°36'	6075							1	*	1	*	1	#*^	379	319	18360425
115	1837	4	11	Alpi Apuane	44°10'	10°15'	6155											1	*	383	320-367	
116	1837	4	12	Cassino	41°30'	13°50'	6156					2	*					1	#*	384	367	
117	1838	6	23	S. Costanzo	43°50'	13°0'	6214											1	#*	385	345	
118	1839	8	26	Montecassino	41°30'	13°50'	6246											1	*		345	
119	1841	2	21	S. Marco	41°40'	15°35'	6874											1	#	390		
120	1841	10	6	Arta	46°25'	13°0'	6943											1	#	392		
121	1841	10	15	Sanguinetto	45°10'	11°10'	6974											1	*		345	
122	1843	10	25	S. Pietro	44°0'	11°15'	7062											1	#*	393	345	
123	1846	8	14	Orciano Pisano	43°30'	10°30'	7160	1	#*	1	*	1	*	1	*			1	#*^	396-397-399	320-321-348	18460814
124	1847	5	8	Medio Tirreno	40°48'	13°26'	7273											1	*		345	
125	1849	2	17	Sinalunga	43°10'	11°45'	7364			2	*										251	
126	1849	11	28	Borgo Val di Taro	44°25'	9°45'	7381											1	#	405		
127	1851	8	14	Vulture	40°59'	15°39'	7534	2	#*^			2	#*	1	*			1	#*	407-409	321	18510814
128	1851	12	30	Reggio Calabria	38°6'	15°39'	7627					1	*					1	*		322-348	
129	1852	12	9	S. Severo	41°40'	15°20'	7843											1	#	412		
130	1853	2	19	Moggio Udinese	46°23'	13°6'	7847											1	#	412		
131	1853	4	9	Caposele	40°50'	15°10'	7941											1	*		322	
132	1853	6	21	Urbino	43°45'	12°40'	8051											1	#	654		
133	1854	2	11	Cosenza	39°18'	16°15'	8097							1	*	1	*	1	#	419	323	
134	1854	2	11	Assisi	43°5'	12°35'	8098									2	*	1	#	416	322	
135	1854	6	16	Castel Bolognese	44°20'	11°45'	8200											1	#	419		
136	1854	12	4	Siena	43°20'	11°20'	8239											1	#	420		
137	1855	5	29	Frascati	41°47'	12°42'	8276											1	#	422		
138	1855	7	25	Vallese	46°18'	7°54'	8304							1	*			1	#*	422	323	18550725
139	1856	10	12	Bovino	41°20'	15°27'	8380									1	*	1	#		324	
140	1857	2	1	Idro	45°45'	10°28'	8399											1	#	424		
141	1857	12	16	Basilicata	40°19'	15°56'	8443	1	*	1	*	1	*	1	*	1	*	1	#*^	430-432	324-325-438	18571216
142	1858	10	25	Cavour	44°50'	7°20'	8677											1	#	432		
143	1859	1	20	Pieve di Soligo	45°54'	12°12'	8704							1	*					325		
144	1859	4	12	Siena	43°20'	11°20'	8754											1	#	435		
145	1859	8	22	Serravalle	42°50'	13°0'	8819					1	*					1	#*	436	325-326	
146	1860	7	19	Valdobbiadene	45°54'	12°3'	8852											1	#	437		
147	1861	3	16	Sesto Godano	44°20'	9°36'	8862											1	#	438		
148	1861	5	9	Città della Pieve	42°55'	12°0'	8865											1	#	438		
149	1861	12	8	Vesuvio	40°49'	14°26'	8911	2	*	2	*	2	*					2	*		261	
150	1864	2	7	Castel D'Aiano	44°20'	11°0'	9082											1	#*	440-441	345	
151	1865	7	19	Etna	37°45'	15°10'	9152			2	^							1	# 2^	442		18650719
152	1865	9	21	Lama	43°35'	12°15'	9187											1	*		345	
153	1866	9	19	Catanzaro	38°54'	16°36'	9232	2	*			2	*								266	
154	1866	11	8	Monte Baldo	45°45'	10°50'	9238											1	#	445		
155	1867	10	3	Mistretta	37°56'	14°22'	9253											1	*		345	
156	1868	5	22	Brenzone	45°40'	10°45'	9284					2	*								268	
157	1868	8	3	Subiaco	41°55'	13°5'	9291	2	*									2	*		268	
158	1869	2	7	Siena	43°20'	11°20'	9301											1	#	446		
159	1869	12	13	Serramazzoni	44°30'	10°45'	9376											1	#	449		
160	1870	10	4	Cosenza	39°18'	16°18'	9450	1	*			1	*	1	*			1	#*	451	327-348	18701004
161	1871	3	24	La Salle	45°42'	6°58'	9673											1	#	455		
162	1871	6	24	Castelletto	44°25'	7°40'	9677											1	*		345	
163	1871	10	17	Acquasparta	42°41'	12°33'	9722											1	#*	456	345	
164	1872	4	26	Castelletto	44°25'	7°40'	9759											1	*		275-345	
165	1872	5	14	Cividale	46°6'	13°26'	9764											1	#	450		
166	1873	3	12	Polverina	43°7'	13°5'	9819							1	*	1	*	1	#*	458	328-329-346	

167	1873	6	29	Bellunese	46°11'	12°23'	9858													2	#*			2	# 1*					1	#*	459-461	329					
168	1873	7	12	Alvito	41°40'	13°44'	9928													1	#			1	#			1	*	1	*	462	330					
169	1875	1	7	Acireale	37°37'	15°10'	10585																							1	#	466						
170	1875	3	17	Cesenatico	44°12'	12°24'	10615																					1	*				331					
171	1875	12	6	S. Marco	41°42'	15°42'	10679																							1	#	469						
172	1876	5	29	S. Marco	41°42'	15°42'	10792																							1	#	471						
173	1877	3	3	Chiusa Verna	43°40'	11°50'	10955																							1	#	472						
174	1878	1	22	Villanova	44°40'	7°30'	11079																							1	#	474						
175	1878	3	26	Terracina	41°17'	13°15'	11097													2	*												278					
176	1879	1	7	Gargano	45°42'	10°40'	11170																							1	#	477						
177	1879	2	23	Serravalle	42°47'	13°3'	11185																							1	#	478						
178	1879	6	17	Etna	37°41'	15°8'	11257													2	^									1	#	480			18790617			
179	1879	8	5	Acireale	37°37'	15°10'	11300																					1	*				346					
180	1880	6	13	Giarre	37°41'	15°7'	11377																							2	*		279					
181	1880	7	23	Brisighella	44°12'	11°48'	11396																					1	*				346					
182	1880	7	24	Medio Tirreno	40°48'	13°26'	11397																							1	#	482						
183	1880	7	24	Medio Tirreno	40°48'	13°28'	11399																					1	*				346					
184	1881	1	24	Pianoro	44°24'	11°27'	11474																							1	#	483						
185	1881	3	4	Isola D'Ischia	40°45'	13°55'	11516	1	*			1	*	1	*			1	#*													486	332-348					
186	1881	3	11	Foligno	42°56'	12°45'	11528																			2	*	1	*	1	*		331					
187	1881	9	10	Lanciano	42°14'	14°24'	11605																							1	#	487						
188	1883	7	28	Casamicciola	40°45'	13°54'	11949											1	ç	1	^			1	^			1	^	1	#^	496			18830728			
189	1885	1	24	Mar Ligure	43°50'	8°0'	12159																							1	#	501						
190	1885	2	10	Mar Ligure	44°20'	9°0'	12167																							1	#	501						
191	1885	9	17	Benevento	41°8'	14°48'	12253																							1	#	502						
192	1885	12	24	La Gretagna	40°30'	16°27'	12321																							1	#	504						
193	1886	9	5	Giaveno	45°5'	7°22'	12794																							1	#	510						
194	1887	1	26	Lucoli	42°20'	13°24'	12839																							1	#	511						
195	1887	2	23	Mar Ligure	43°42'	8°3'	12870																							1	^				18870223			
196	1887	5	20	Oggiano	45°50'	9°24'	12933																							1	#	516						
197	1887	11	9	Predappio	44°9'	12°3'	12986																							1	#	519						
198	1887	11	14	Impruneta	43°44'	11°16'	12993																							1	#	519						
199	1887	12	14	Bormio	46°30'	10°22'	13011																							1	#	522						
200	1891	1	20	Vallese	46°15'	7°15'	13571																							1	#	533						
201	1891	6	7	Tregnago	45°32'	11°9'	13599													2	^									2	^	535			18910607			
202	1891	10	15	Canale di Sicilia	36°45'	12°0'	13675																							1	#	538						
203	1892	3	5	Bard	45°37'	7°47'	14112																									542						
204	1892	11	15	Medio Tirreno	40°56'	12°52'	14523																							1	#	548-549						
205	1894	3	25	Lesina	41°51'	15°22'	14852																							1	#	563						
206	1894	11	16	Bagnara Calabra	38°18'	15°48'	14962													1	^			1	^	1	^			2	#	567-570			18941116			
207	1895	3	23	Comacchio	44°42'	12°11'	15231																							1	#	574						
208	1895	4	14	Ljbjana	46°6'	14°30'	15294																							1	#	577						
209	1897	12	6	Lago Ampollino	39°15'	16°42'	16272																							1	#	609						
210	1897	12	18	Lama	43°32'	12°15'	16303																	1	#	1	#	1	#	1	#	609						
211	1898	1	16	Argenta	44°37'	11°51'	16363																									612						
212	1898	2	20	Cividale	46°6'	13°27'	16423																							1	#	614						
213	1898	3	4	Calestano	44°38'	10°10'	16459																							1	#	616-663						
214	1898	6	29	Rieti	42°23'	12°54'	16620																							1	#	619						
215	1905	9	8	Golfo di S. Eufemia	38°48'	16°6'	19344													1	^			1	^					1	^				19050908			
216	1917	4	26	Monterchi	43°29'	12°7'	26049													2	^			1	^					1	^				19170426			
217	1968	1	15	Valle del Belice	37°42'	13°6'	35810													1	^	1	^	1	^					1	^				19680115			
218	1976	5	6	Lusevera	46°16'	13°14'	38942													2	^			2	^										19760506			
219	1980	11	23	Irpinia - Lucania	40°48'	15°22'	41752													1	§			1	§			1	§									

Table S.2. Catalogue of all fluid-related or ground deformative precursory phenomena that occurred throughout the world in the period of 1948-2009. These phenomena were described in previous catalogues compiled by Hauksson (1981), Friedmann (1985),Toutain and Baubron (1990), Kissin and Grinevsky (1990), Hartmann and Levy (2005), Roeloffs (2006), Gosh et al. (2009), Cicerone et al. (2009), Petraki et al. (2015) and Woith (2015), in which a variety of papers on earthquake precursors were reviewed. The merging of previous catalogues allowed the compilation of an updated catalogue.

Country	Geographyc area of seismic event	Type of precursor	Hauksson, 1981	Friedmann, 1985	Kissin and Grinevsky, 1990	Roeloffs, 2006	Cicerone et al., 2009	Ghosh et al., 2009	Petraki et al., 2015
Algeria	Boumerdes	gas emissions variations							X
Antartide	Vernadsky Research Base	gas emissions variations						X	
Antartide	Orcadas Research Base	gas emissions variations							X
Armenia	Arax basin	gas emissions variations						X	
Austria	Judenburg	gas emissions variations		X					
Columbia	Quindio	gas emissions variations						X	
Croatia	Modrica	gas emissions variations						X	
Ecuador	Reventador	gas emissions variations					X		X
Former Jugoslavija	Montenegro	gas emissions variations		X					
Former USSR	Caucasus	gas emissions variations						X	
Former USSR	Alma-Ata	gas emissions variations	X				X		X
Former USSR	Duchambe	gas emissions variations					X		
Former USSR	Gazli	gas emissions variations	X	X			X		X
Former USSR	Iran	gas emissions variations					X		
Former USSR	Isfarin-Batnen	gas emissions variations	X				X		X
Former USSR	Markansu	gas emissions variations	X				X		X
Former USSR	Taschkent	gas emissions variations	X				X		X
Former USSR	Tien Shan	gas emissions variations	X				X		X

Former USSR	Turkmenistan	gas emissions variations				X
Former USSR	Uzbekistan	gas emissions variations	X	X		X
Former USSR	Zaalai	gas emissions variations	X	X		X
France	Eastern Pyrenees	gas emissions variations		X		
France	Marictims Alps	gas emissions variations		X		X
France	Perpignan	gas emissions variations		X		
Greece	Chalkida, Evia Island	gas emissions variations				X
Greece	Kato Achaia, Peloponnese	gas emissions variations				X
Greece	Mytilene, Lesvos Island	gas emissions variations				X
Iceland	Southern	gas emissions variations	X	X		X
Iceland	Tjörnes Facture Zone	gas emissions variations	X	X		X
India	Chamoli	gas emissions variations		X	X	X
India	N-W Himalaya	gas emissions variations			X	
India	Chamba	gas emissions variations				X
India	Dharamsala	gas emissions variations				X
India	Himachal Pradesh	gas emissions variations		X		X
India	Hindu Kush area	gas emissions variations				X
India	Kangra Valley	gas emissions variations				X
India	Kharsali	gas emissions variations				X
India	Maheshwaram	gas emissions variations		X		X
India	North Andaman	gas emissions variations				X
India	Sunder Nagar	gas emissions variations				X
India	Theri Garhwal	gas emissions variations				X
India	Uttarkashi	gas emissions variations		X		X
Indonesia	Indonesia	gas emissions variations				X
Indonesia	North Sumatra	gas emissions variations				X
Indonesia	West Sumatra	gas emissions variations				X
Iran	Jooshan	gas emissions variations				X
Italy	Rome	gas emissions variations			X	
Italy	Irpinia	gas emissions variations		X		
Italy	Monte Etna	gas emissions variations				X
Japan	Izu Peninsula	gas emissions variations			X	
Japan	Byakko	gas emissions variations		X		

Japan	Chiba-Ken-Oki	gas emissions variations					X		
Japan	Fukushima	gas emissions variations					X		X
Japan	Hyogo-Ken Nambu Zisin	gas emissions variations					X		
Japan	Izu–Oshima	gas emissions variations	X				X		X
Japan	Kobe	gas emissions variations					X		X
Japan	Matsuyama area	gas emissions variations					X		
Japan	Nagoya	gas emissions variations					X		
Japan	Subducted zone	gas emissions variations					X		X
Japan	Western Nagano	gas emissions variations					X		
Mexico	Acapulco	gas emissions variations						X	
Mexico	Mexico	gas emissions variations					X		
Philippines	Mindoro	gas emissions variations					X		X
PR China	Cangzui	gas emissions variations	X						
PR China	Chienan	gas emissions variations	X				X		X
PR China	Fengzhen	gas emissions variations					X		
PR China	Haicheng	gas emissions variations	X	X			X		X
PR China	Hsingtang	gas emissions variations	X				X		X
PR China	Liaoyang	gas emissions variations					X		X
PR China	Luhuo	gas emissions variations	X	X			X		X
PR China	Lungling	gas emissions variations	X	X			X		X
PR China	Mapien	gas emissions variations	X	X			X		X
PR China	Ninghe	gas emissions variations		X			X		
PR China	Ningshin	gas emissions variations	X				X		X
PR China	Pan Shan	gas emissions variations	X						
PR China	Peking	gas emissions variations	X						
PR China	Pohai Bay	gas emissions variations	X				X		X
PR China	Sabteh	gas emissions variations	X				X		X
PR China	Songpan	gas emissions variations	X	X			X		X
PR China	Songpan-Pingwu	gas emissions variations	X				X		X
PR China	Takung	gas emissions variations	X				X		X
PR China	Tangshan	gas emissions variations	X	X			X		X
PR China	Yiliang	gas emissions variations	X				X		X
Romania	Vrancea seismic area	gas emissions variations					X		

Russia	Kamchatka Peninsula	gas emissions variations					X		
Slovenia	Grmada	gas emissions variations						X	X
Slovenia	Kremen	gas emissions variations						X	X
Slovenia	Krško	gas emissions variations						X	X
Spain	Galicia	gas emissions variations					X		
Spain	Tenerife Island	gas emissions variations							X
Taiwan	Taiwan	gas emissions variations					X	X	X
Taiwan	Northern Taiwan	gas emissions variations					X		X
Thailand	Thailand	gas emissions variations						X	
Turkey	Turkey	gas emissions variations						X	X
United Kingdom	Dudley	gas emissions variations							X
United Kingdom	English Channel	gas emissions variations							X
United Kingdom	Manchester	gas emissions variations							X
USA	Alandale	gas emissions variations					X		X
USA	Big Bear	gas emissions variations	X				X		X
USA	Blue Mountain Lake	gas emissions variations					X		X
USA	Caruthersville, Missouri	gas emissions variations					X		X
USA	Central Arkansas	gas emissions variations					X		X
USA	Coalinga fault	gas emissions variations					X		
USA	Coyote Lake, California	gas emissions variations					X		
USA	Hollister, California	gas emissions variations					X		
USA	Imperial Valley	gas emissions variations	X	X			X		X
USA	Jocasse	gas emissions variations	X				X		X
USA	Kettleman Hill	gas emissions variations					X		X
USA	Livermore, California	gas emissions variations					X		
USA	Loma Prieta, California	gas emissions variations					X		
USA	Malibu	gas emissions variations	X				X		X
USA	Mt Diablo, California	gas emissions variations					X		
USA	New Madrid Seismic Zone	gas emissions variations					X		X
USA	Pasadena	gas emissions variations	X				X		X
USA	Pearblossom	gas emissions variations	X				X		X
USA	Raquette Lake	gas emissions variations					X		X
USA	Salinas, California	gas emissions variations					X		

USA	San Andreas fault, California	gas emissions variations		X		X
USA	San Bernardino, California	gas emissions variations				X
USA	San Juan Bautista, California	gas emissions variations		X		
USA	Sand Point, Alaska	gas emissions variations		X		
USA	SW Illinois	gas emissions variations		X		X
USSR	Abrau-Dyurso	gas emissions variations			X	
USSR	Pyatigorsk	gas emissions variations			X	
USSR	Sakhalin	gas emissions variations			X	
USSR	Paravani, Caucasus	gas emissions variations		X		
USSR	Spitak, Caucasus	gas emissions variations		X		
Armenia	Spitak	ground deformation		X		
Chile	Chile	ground deformation	X			
Greece	Corinth Rift	ground deformation	X			
Italy	Central Appenines	ground deformation		X		
Italy	Friuli	ground deformation		X		
Italy	Irpinia	ground deformation		X		
Japan	Izu–Oshima	ground deformation		X		
Japan	Izu-Oshima-Kinkai	ground deformation	X			
Japan	Japan Sea	ground deformation	X			
Japan	Japan Sea	ground deformation		X		
Japan	Nankaido	ground deformation	X			
Japan	Niigata	ground deformation		X		
Japan	Tonankai	ground deformation	X			
Japan	Tonankai	ground deformation		X		
Japan	Urakawa-oki, Japan	ground deformation	X			
Peru	Peru	ground deformation	X			
Russia	Kamchatka Gulf	ground deformation		X		
USA	Big Bear, California	ground deformation		X		
USA	Briones Hills, California	ground deformation		X		
USA	Calaveras Fault, California	ground deformation		X		
USA	Hollister, Calfiornia	ground deformation		X		
USA	Homestead Valley, California	ground deformation		X		
USA	Joshua Tree, California	ground deformation		X		

USA	Kalapana, Hawaii	ground deformation			X
USA	Kettleman Hills, California	ground deformation		X	
USA	Landers, California	ground deformation			X
USA	Loma Prieta, California	ground deformation			X
USA	Lytle Creek, California	ground deformation			X
USA	Prince William Sound, Alaska	ground deformation		X	
USA	San Andreas Fault, California	ground deformation			X
USA and Canada	Cascadia	ground deformation		X	
Afghanistan	Hindu Kush	groundwater level variations	X		X
China	Hebei	groundwater level variations	X		X
China	Liaoning	groundwater level variations	X		X
China	Singhai	groundwater level variations	X		X
Former USSR	Baykal area	groundwater level variations	X		X
Former USSR	Kazakhstan	groundwater level variations			X
Former USSR	Kirgizia	groundwater level variations	X		X
Former USSR	Kuril Islands	groundwater level variations	X		X
Former USSR	Tadzhikistan	groundwater level variations	X		X
Former USSR	Turkmenistan	groundwater level variations	X		X
Former USSR	Uzbekistan	groundwater level variations	X		X
Greece	Thessaloniki	groundwater level variations			X
India	Koyna-Warna	groundwater level variations			X
Iran	Lutt Plateau	groundwater level variations	X		X
Japan	Hokkaido	groundwater level variations			X
Japan	Izu Peninsula	groundwater level variations	X		X
Japan	Izu–Oshima–kinkai	groundwater level variations			X
Japan	Sanriku	groundwater level variations			X
Japan	southwest Japan	groundwater level variations			X
Japan	Tokyo Bay	groundwater level variations			X
Japan	Tono Mine	groundwater level variations			X
Taiwan	Taiwan	groundwater level variations			X
USA	California	groundwater level variations	X		X
USA	Kettleman Hills	groundwater level variations			X
USA	San Jacinto, California	groundwater level variations			X

China	Datong	temperature variations	X
Greece	Bay of Patras	temperature variations	X
Greece	Thessaloniki	temperature variations	X
Japan	Ibaraki–Ken–Oki	temperature variations	X
Japan	Ito–Oki	temperature variations	X
Japan	Izu–Hanto–Toho–Oki	temperature variations	X
Japan	Izu–Oshima–Kinkai	temperature variations	X
Japan	Kawazu	temperature variations	X
Japan	Miyagi–Ken–Oki	temperature variations	X
Japan	Sagami Bay	temperature variations	X
USA	Loma Prieta, California	temperature variations	X
USA	Morgan Hill, California	temperature variations	X
USA	Oroville, California	temperature variations	X